# Stably Stratified Atmospheric Turbulence and Internal Gravity Waves


**Igor Rogachevskii, Tov Elperin, Nathan Kleeorin,**

*Ben-Gurion University of the Negev, Beer-Sheva, Israel*

***NORDITA, KTH Royal Institute of Technology and Stockholm University, Sweden***

**Sergej Zilitinkevich**

*University of Helsinki and Finnish Meteorological Institute, Helsinki, Finland*

**Victor L'vov**

מכון ויצמן למדע

WEIZMANN INSTITUTE OF SCIENCE

*Rehovot, Israel*

# Outline

## Energy and Flux Budget Turbulence Closure Theory

- **Atmospheric Sheared Stably Stratified Turbulence without Waves**
- **Atmospheric Sheared Stably Stratified Turbulence with Internal Gravity Waves**
- **Atmospheric Shear Free Stably Stratified Turbulence produced by Internal Gravity Waves**
- **Laboratory Experiments (Stably Stratified Turbulence)**
- **Atmospheric Turbulent Convection (may be)**

# Stable PBL

Shallow, stably-stratified planetary boundary layer (PBL) in Bergen visualized by water haze (winter 2012, courtesy T. Wolf)

# Budget Equation for TKE

$$\frac{\partial E_K}{\partial t} = \Pi_{tot} - T - D$$

$$E_K = \frac{1}{2}\langle \mathbf{u}^2 \rangle$$

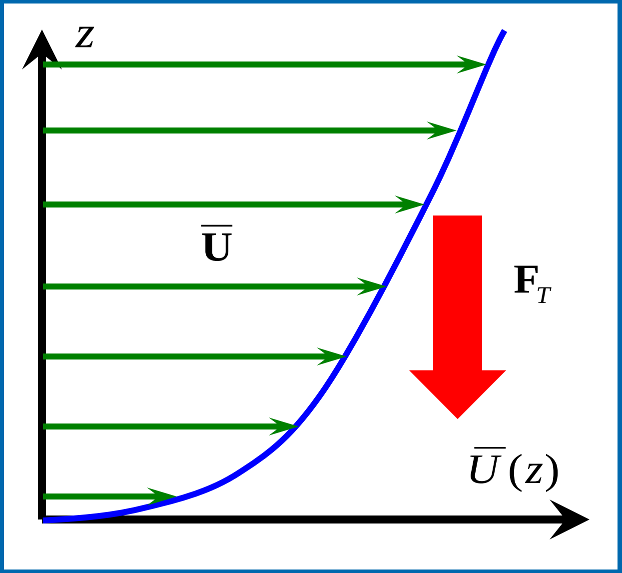


**Balance in R-space**

$$\Pi_{tot} \approx D$$

$$\mathbf{S} = \frac{\partial \bar{\mathbf{U}}}{\partial z}$$

$$T = \mathrm{div}\, \mathbf{\Phi}_u$$

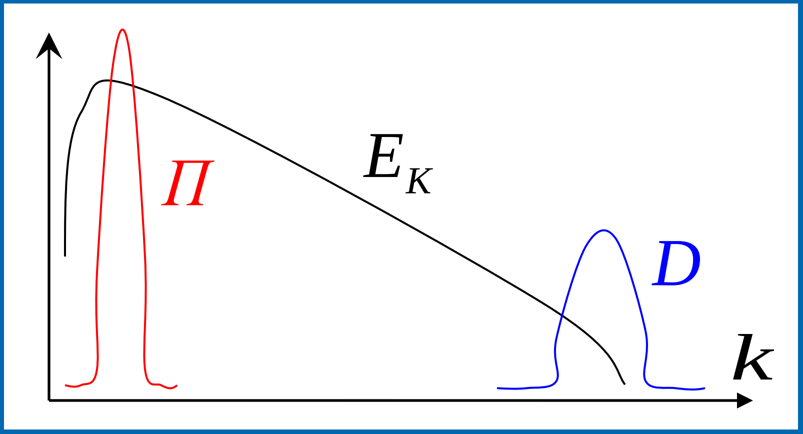


$$\frac{\partial E_K}{\partial t} = K_M S^2 - \beta |F_z| - \frac{E_K}{t_T} - T$$

$$\Pi = -\langle u_i u_j \rangle \nabla_j \bar{U}_i = K_M S^2$$

**Steady-state for homogeneous turbulence:**

$$t_T = \frac{l}{\sqrt{E_K}} \qquad \mathrm{Ri} = \frac{N^2}{S^2} \qquad N^2 = \beta \frac{\partial \bar{\Theta}}{\partial z}$$

$$E_K \approx t_T (K_M S^2 - \beta |F_z|)$$

# TKE Balance for SBL

$$\frac{\partial E_K}{\partial t} = K_M S^2 - \beta \,|\, F_z \,|\, - \frac{E_K}{t_T} - T$$

$$\begin{array}{ccccc} \boxed{S} & \longrightarrow & \boxed{TKE} & \longrightarrow & \boxed{D_U} \\ & & \downarrow & & \\ & & \boxed{B} & & \end{array}$$

$$E_K \approx t_T \left( K_M S^2 - \beta \,|\, F_z \,|\right)$$

$$"S" = "B"$$

$$\downarrow$$

$$\mathrm{Ri}_C \approx 0.25$$

$$B \equiv \beta F_z = -(2E_z t_T) \frac{\partial \bar{\Theta}}{\partial z}$$

$$\beta = \frac{g}{T_0}$$

$$\mathrm{Ri} = \frac{N^2}{S^2}$$

$$N^2 = \beta \frac{\partial \overline{\Theta}}{\partial z}$$

$$\Theta = T (P_0 / P)^{1-1/\gamma}$$

# Budget Equations for SBL

- Turbulent kinetic energy: $E_K = \frac{1}{2}\langle \mathbf{u}^2 \rangle$
- Potential temperature fluctuations: $E_\theta = \frac{1}{2}\langle \theta^2 \rangle$
- Flux of potential temperature : $\mathbf{F} = \langle \mathbf{u}\,\theta \rangle$

$$\frac{DE_K}{Dt} + \operatorname{div}(\mathbf{\Phi}_u) - \Pi - \beta F_z = -D_K$$

$$\frac{DE_\theta}{Dt} + \operatorname{div}(\mathbf{\Phi}_\theta) + \frac{N^2}{\beta} F_z = -D_\theta$$

$$\frac{DF_i}{Dt} + \operatorname{div}_j(\Phi^F_{ij}) + (\mathbf{F}\cdot\nabla)\overline{U}_i + \frac{N^2}{\beta}\tau_{ij}e_j - 2C_\theta \beta e_i E_\theta = -D^F_i$$

$$D_K = \frac{E_K}{t_T} \qquad D_\theta = \frac{E_\theta}{C_\theta t_T} \qquad D^F_i = \frac{F_i}{C_F t_T}$$

$$C_\theta \beta_i \langle \theta^2 \rangle = \beta_i \langle \theta^2 \rangle + \frac{1}{\rho_0}\langle \theta \nabla_i p \rangle$$

$$\Pi = -\tau_{ij}\nabla_j \overline{U}_i = K_M S^2$$

# Boussinesq Approximation

$$\left(\frac{\partial}{\partial t}+\mathbf{u}\cdot\vec{\nabla}\right)\mathbf{u}=-\vec{\nabla}\left(\frac{p}{\rho_0}\right)-\boldsymbol{\beta}\,\theta+\nu\,\Delta\mathbf{u}$$

$$\boldsymbol{\beta}=\frac{\mathbf{g}}{T_0}$$

$$\left(\frac{\partial}{\partial t}+\mathbf{u}\cdot\vec{\nabla}\right)\theta=\kappa\,\Delta\theta-\mathbf{u}\cdot\vec{\nabla}\overline{\Theta}$$

$$\theta=T\left(\frac{p_0}{p}\right)^{(\gamma-1)/\gamma}$$

$$\vec{\nabla}p_0=\rho_0\mathbf{g}$$

$$\frac{\text{inertial force}}{\text{viscous force}}\propto\frac{\mathrm{u}\,\ell}{\nu}=\mathrm{Re}\approx10^6\div10^7$$

$$\frac{\text{advective term}}{\text{diffusive term}}\propto\frac{\mathrm{u}\,\ell}{\kappa}=\mathrm{Pe}\approx10^6\div10^7$$

# Budget Equations for SBL

$$\frac{DE_K}{Dt} + \frac{\partial \Phi_K}{\partial z} = \Pi + \beta F_z - D_K$$

$$\frac{DE_P}{Dt} + \frac{\partial \Phi_P}{\partial z} = - \beta F_z - D_P$$

$$E_\theta = \frac{1}{2} \left\langle \theta^2 \right\rangle$$

$$D_K = \frac{E_K}{t_T}$$

$$D_P = \frac{E_P}{C_P \, t_T}$$

$$E_p \equiv \frac{g}{\rho_0} \left\langle \int \rho \, dz \right\rangle = \left( \frac{\beta}{N} \right)^2 E_\theta = \frac{1}{2} \left( \frac{\beta}{N} \right)^2 \left\langle \theta^2 \right\rangle$$

# Total Turbulent Energy

$$\frac{DE}{Dt} + \nabla \cdot \mathbf{\Phi} = \Pi - \frac{E}{C_u \, t_T}$$

$$E = E_K + \left(\frac{\beta}{N}\right)^2 E_\theta$$

The turbulent potential energy:

$$\boxed{E_P = \left(\frac{\beta}{N}\right)^2 E_\theta}$$

Production of Turbulent energy:

$$\Pi = -\tau_{ij} \nabla_j \bar{U}_i = K_M S^2$$

$$K_M = 2 C_\tau A_z l \sqrt{E_K}$$

# Budget Equations for SBL

$$\frac{DE_K}{Dt} + \frac{\partial \Phi_K}{\partial z} = \Pi + \beta F_z - D_K$$

$$\frac{DE_P}{Dt} + \frac{\partial \Phi_P}{\partial z} = -\beta F_z - D_P$$

$$\frac{DF_z}{Dt} + \frac{\partial \Phi_F}{\partial z} = -D_z^F - \langle u_z u_z \rangle \frac{\partial \overline{\Theta}}{\partial z} + 2C_\theta \beta E_\theta$$

$$E_p \equiv (\beta / N)^2 E_\theta = ½(\beta / N)^2 \overline{\theta'^2}$$

$$C_\theta \beta_i \langle \theta^2 \rangle = \beta_i \langle \theta^2 \rangle + \frac{1}{\rho_0} \langle \theta \nabla_i p \rangle$$

# No Critical Richardson Number

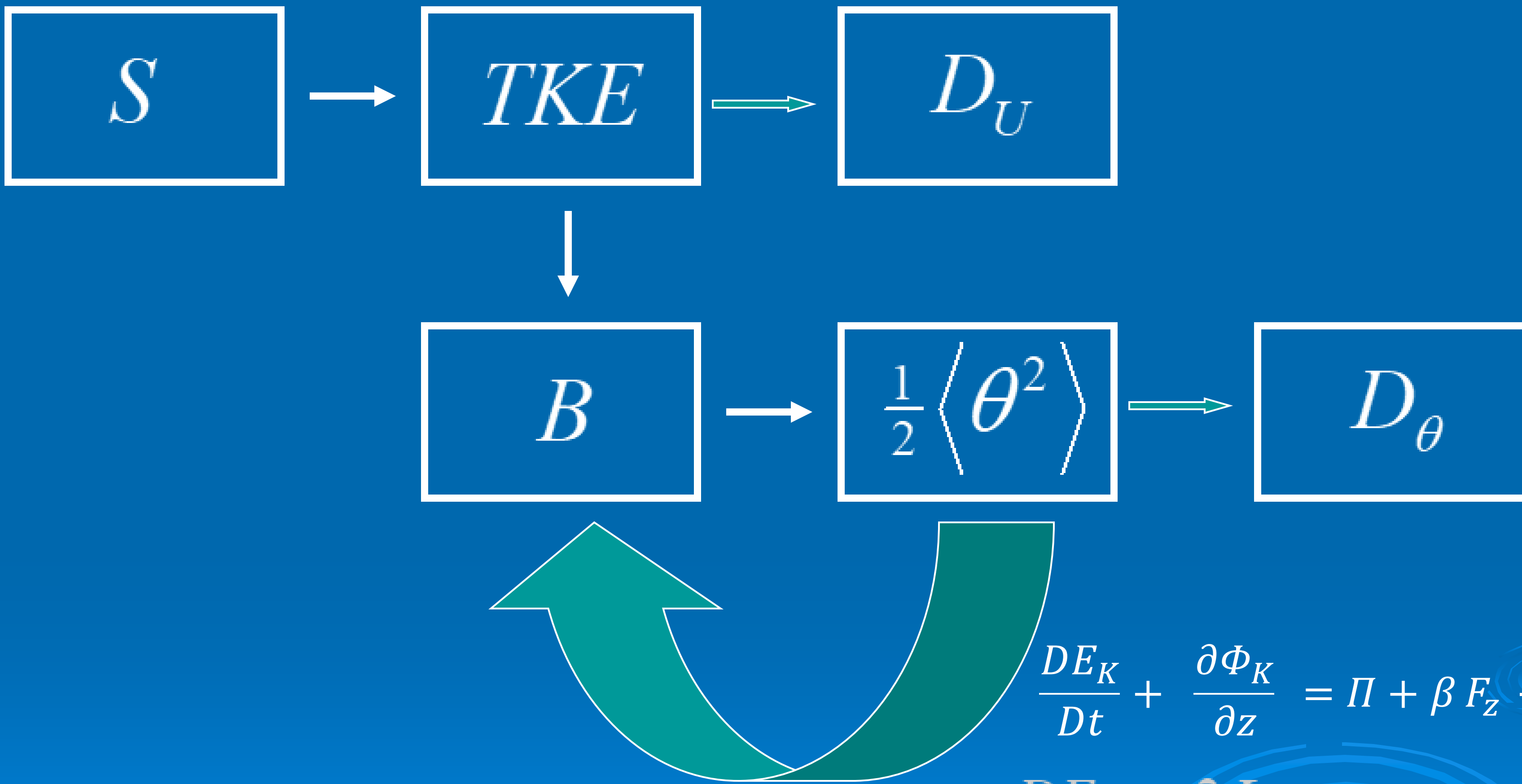


$$\frac{DE_K}{Dt} + \frac{\partial \Phi_K}{\partial z} = \Pi + \beta F_z - D_K$$

$$\frac{DE_P}{Dt} + \frac{\partial \Phi_P}{\partial z} = -\beta F_z - D_P$$

$$B \equiv \beta F_z = -(2E_z t_T)\frac{\partial \bar{\Theta}}{\partial z} + C_\theta \beta^2 \left\langle \theta^2 \right\rangle t_T$$

$$C_\theta \beta_i \left\langle \theta^2 \right\rangle = \beta_i \left\langle \theta^2 \right\rangle + \frac{1}{\rho_0}\left\langle \theta \nabla_i p \right\rangle$$

# Budget Equations for SBL

$$\frac{DE_K}{Dt}+\frac{\partial\Phi_K}{\partial z}=\Pi+\beta F_z-D_K$$

$$\frac{DE_P}{Dt}+\frac{\partial\Phi_P}{\partial z}=-\beta F_z-D_P$$

$$\frac{DF_z}{Dt}+\frac{\partial\Phi_F}{\partial z}=-\left\langle u_z^2\right\rangle\frac{\partial\bar{\Theta}}{\partial z}+2C_\theta\beta E_\theta-\frac{F_z}{C_F t_T}$$

$$E_p\equiv(\beta/N)^2E_\theta=\tfrac{1}{2}(\beta/N)^2\overline{\theta'^2}$$

$$C_\theta\beta_i\left\langle\theta^2\right\rangle=\beta_i\left\langle\theta^2\right\rangle+\frac{1}{\rho_0}\left\langle\theta\nabla_i p\right\rangle$$

# Comparisons

$$Ri = Pr_T Ri_f = \frac{C_\tau}{C_F} Ri_f \left(1 - \frac{Ri_f (1 - R_\infty) A_z^{(\infty)}}{R_\infty (1 - Ri_f) A_z(Ri_f)}\right)^{-1}$$

$$\mathrm{Ri}_f \equiv -\frac{\beta F_z}{\Pi}$$

$$\mathrm{Ri} = \frac{N^2}{S^2}$$

$$\mathrm{Pr}_T \equiv \frac{K_M}{K_H}$$

$$Pr_T \approx Pr_T^{(0)} + \frac{(1 - R_\infty) A_z^{(\infty)}}{R_\infty A_z^{(0)}} Ri.$$

$$Pr_T \approx 0.8 + 0.45 Ri$$

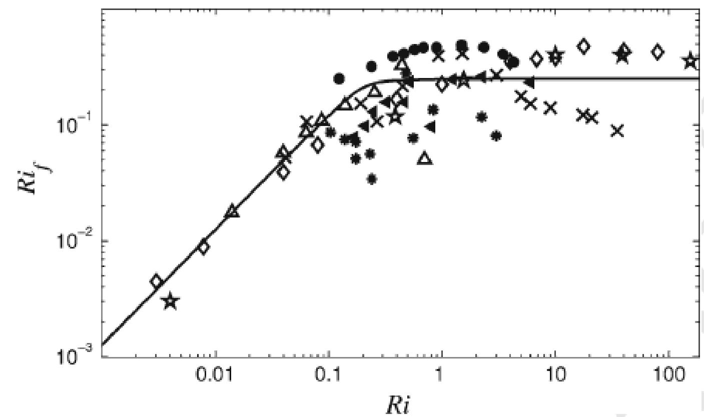


**Fig. 4** *Ri*-dependence of the flux Richardson number $Ri_f = -\beta F_z/(\tau S)$ for *meteorological observations*: *slanting black triangles* (Kondo et al. 1978), *snowflakes* (Bertin et al. 1997); *laboratory experiments*: *slanting crosses* (Rehmann and Koseff 2004), *diamonds* (Ohya 2001), *black circles* (Strang and Fernando 2001); *DNS*: *five-pointed stars* (Stretch et al. 2001); *LES*: *triangles* (our DATABASE64). *Solid line* shows the steady-state EFB model, Eq. 56, with $Ri_f \to R_\infty = 0.25$ at $Ri \to \infty$

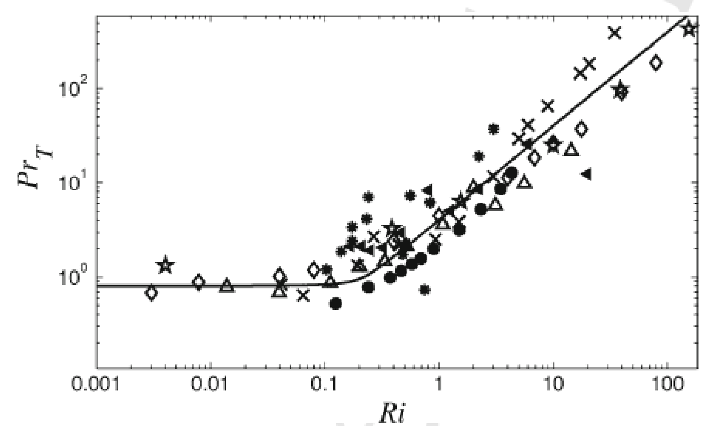


**Fig. 5** *Ri*-dependence of the turbulent Prandtl number $Pr_T = K_M/K_H$, after the same data as in Fig. 4 (meteorological observations, laboratory experiments, DNS, and LES). Solid line shows the steady-state EFB model, Eq. 56

# Comparisons

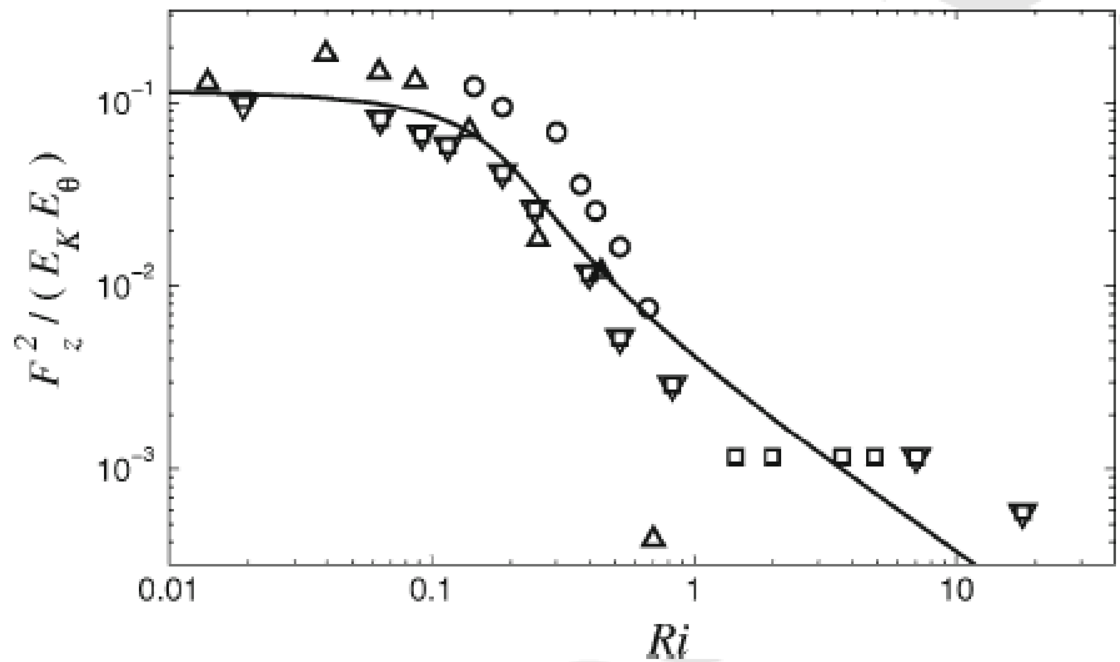


**Fig. 9** *Ri*-dependence of the squared dimensionless turbulent flux of potential temperature $F_z^2/(E_K E_\theta)$, for *meteorological observations*: *squares* (CME), *circles* (SHEBA), *overturned triangles* (CASES-99); *laboratory experiments*: *diamonds* (Ohya 2001); LES: *triangles* (our DATABASE64). *Solid line* shows the steady-state EFB model, Eq. 61

$$\mathrm{Ri} = \frac{N^2}{S^2}$$

$$\frac{F_z^2}{E_K E_\theta} = \frac{2C_\tau}{C_P} \frac{A_z(Ri_f)}{Pr_T}.$$

# Comparisons

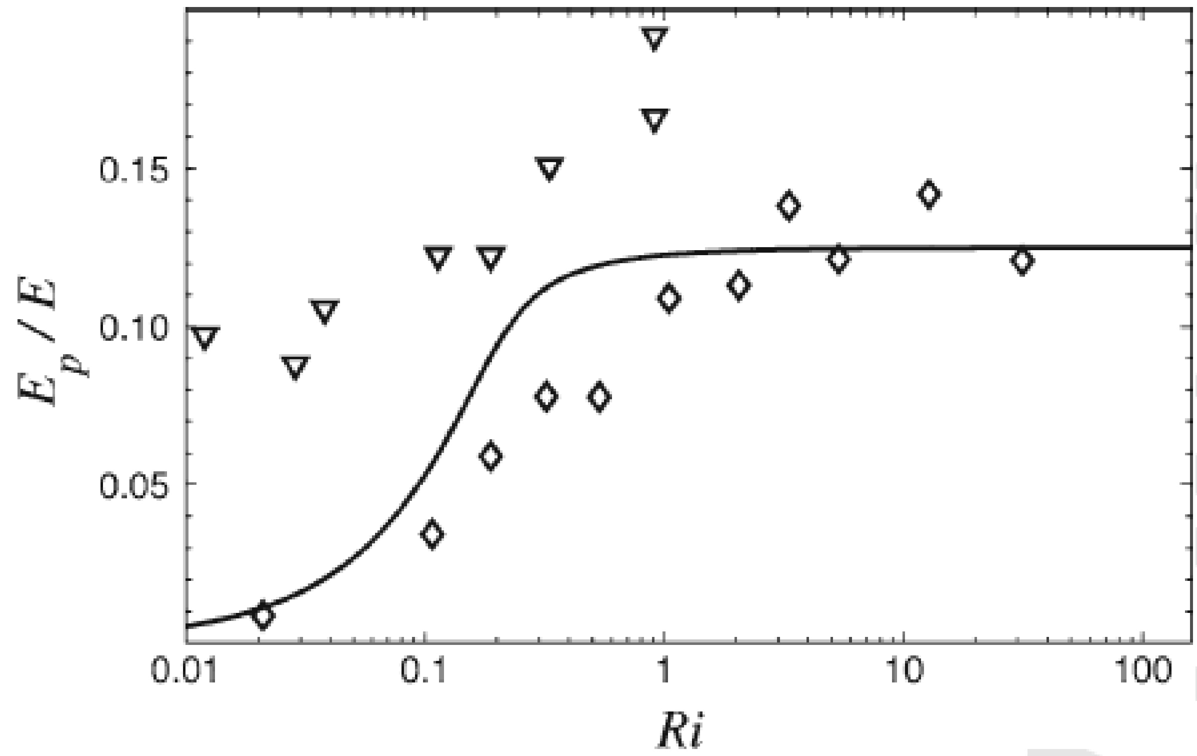


**Fig. 7** *Ri*-dependence of the potential-to-total turbulent energy ratio $E_{\mathrm{P}}/E$, for *meteorological observations: overturned triangles* (CASES-99), and *laboratory experiments: diamonds* (Ohya 2001). *Solid line* shows the steady-state EFB model, Eqs. 54, 56

$$\frac{E_{\mathrm{P}}}{E} = \frac{C_{\mathrm{P}} Ri_{\mathrm{f}}}{1 - (1 - C_{\mathrm{P}}) Ri_{\mathrm{f}}}.$$

$$E = E_K + E_p$$

$$\mathrm{Ri} = \frac{N^2}{S^2}$$

$$Ri = Pr_{\mathrm{T}} Ri_{\mathrm{f}} = \frac{C_\tau}{C_{\mathrm{F}}} Ri_{\mathrm{f}} \left( 1 - \frac{Ri_{\mathrm{f}}(1 - R_\infty) A_z^{(\infty)}}{R_\infty (1 - Ri_{\mathrm{f}}) A_z(Ri_{\mathrm{f}})} \right)^{-1}$$

# Comparisons

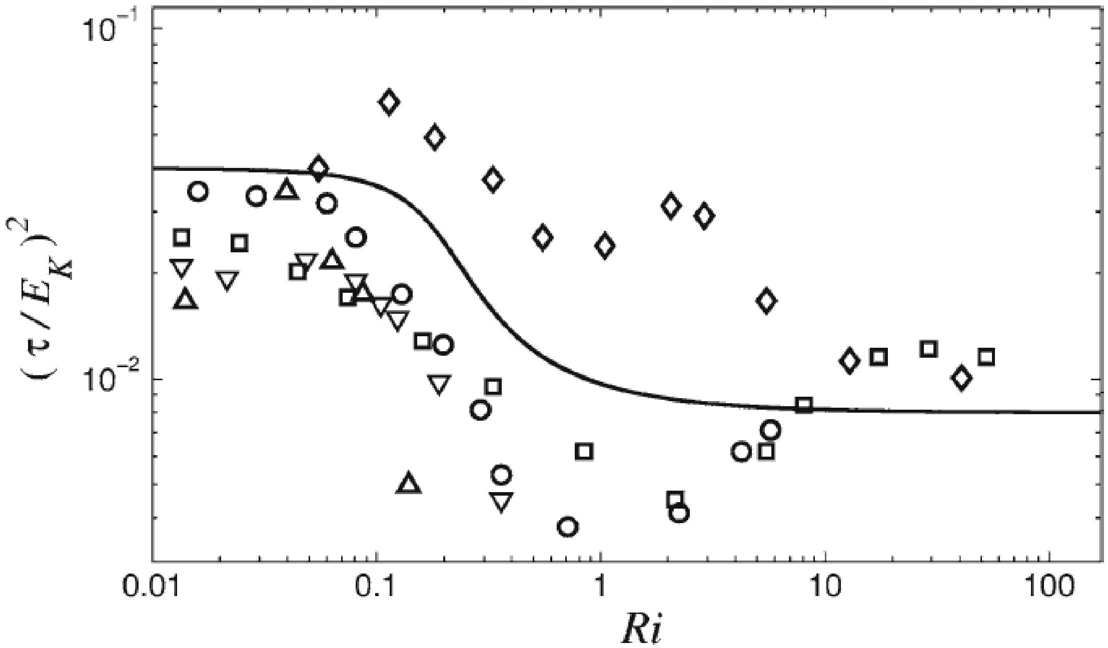


**Fig. 8** *Ri* dependence of the squared dimensionless turbulent flux of momentum $(\tau/E_K)^2$, for *meteorological observations*: *squares* (CME), *circles* (SHEBA), *overturned triangles* (CASES-99); *laboratory experiments*: *diamonds* (Ohya 2001); LES: *triangles* (our DATABASE64). *Solid line* shows the steady-state EFB model, Eq. 60

$$\left(\frac{\tau}{E_K}\right)^2 = \frac{2C_\tau A_z(Ri_f)}{(1 - Ri_f)},$$

$$\tau_{i3} = -K_M \frac{\partial U_i}{\partial z}$$

$$Ri = Pr_T Ri_f = \frac{C_\tau}{C_F} Ri_f \left(1 - \frac{Ri_f (1 - R_\infty) A_z^{(\infty)}}{R_\infty (1 - Ri_f) A_z(Ri_f)}\right)^{-1}$$

# Comparisons

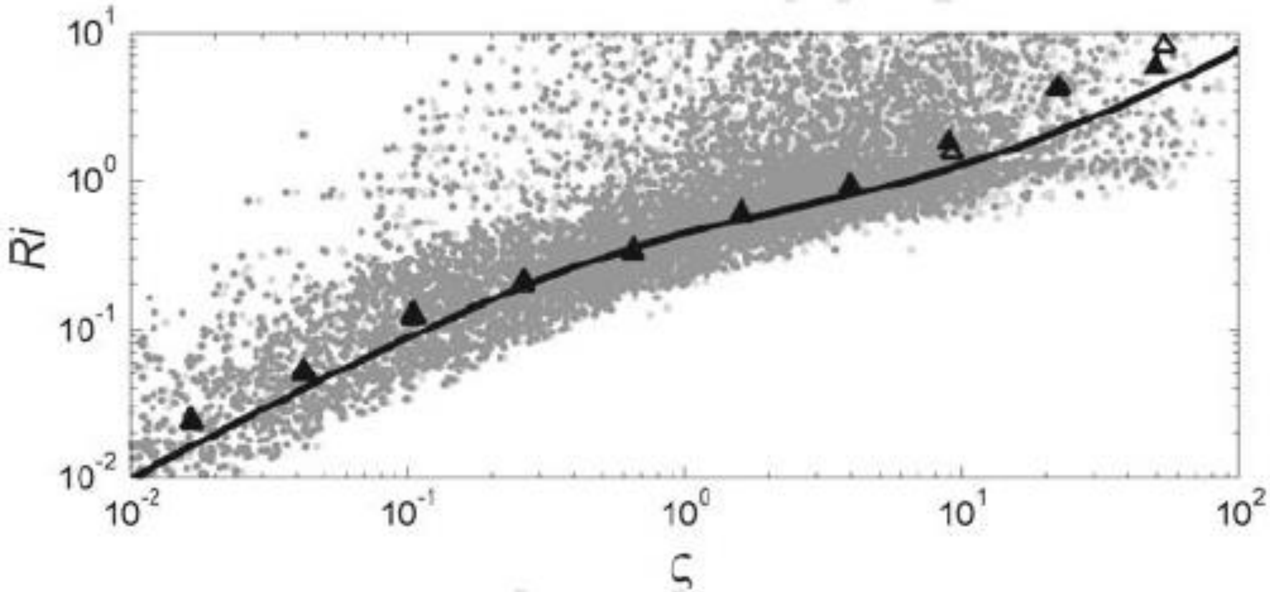


**Fig. 12** Gradient Richardson number *Ri* versus dimensionless parameters $\varsigma = z/L$ (*white triangles*) and $\varsigma = l_0/L$ (*black triangles*) based on the Obukhov length scale $L$, after our LES. *Solid line* shows our model. *Open triangles* correspond to $\varsigma = z/L$, *black triangles* to $\varsigma = z/[(1 + C_\Omega \Omega z/E_K^{1/2})L]$

$$Ri \equiv \frac{N^2}{S^2},$$

$$L = \frac{\tau^{3/2}}{-\beta F_z}$$

$$K_M = \tau/S$$

# Comparisons

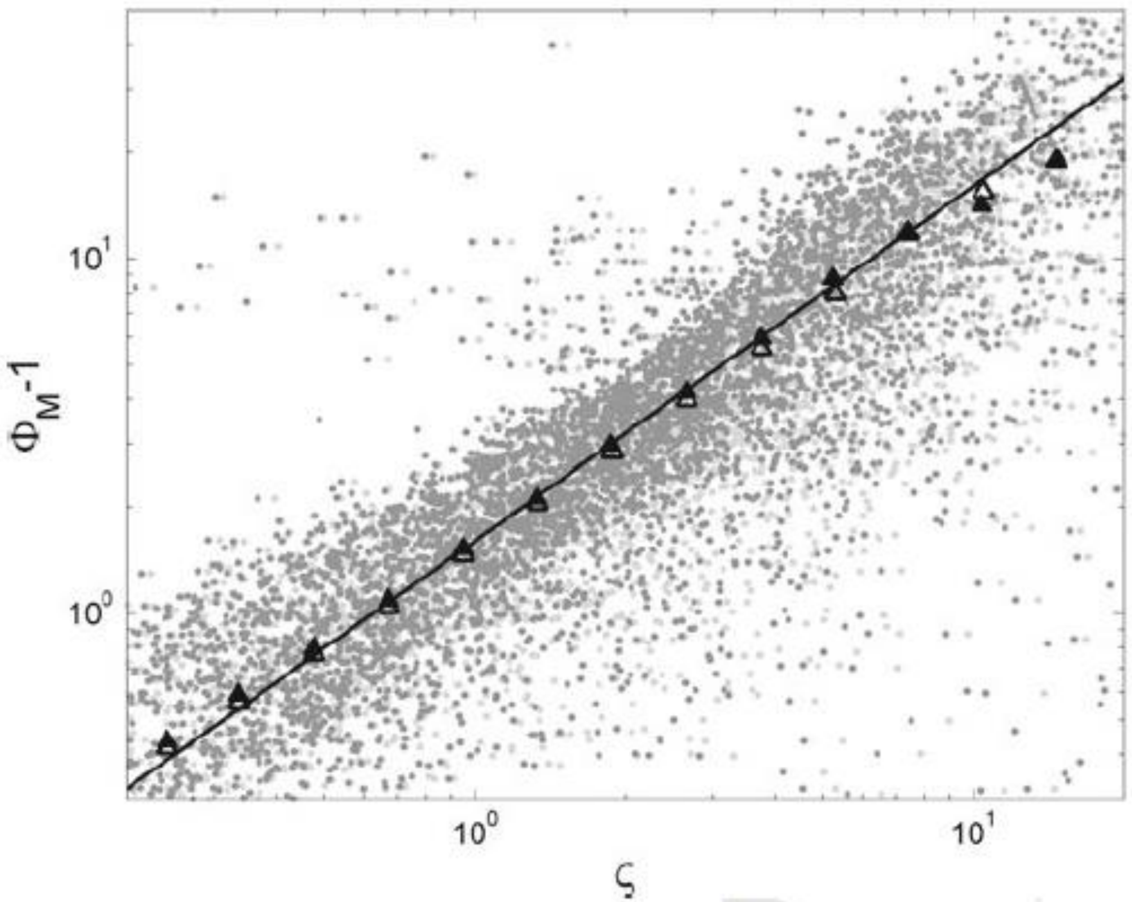


**Fig. 10** Dimensionless wind-velocity gradient $\Phi_M = (kz/\tau^{1/2})(\partial U/\partial z)$ versus dimensionless height $\varsigma$ based on the Obukhov length $L$ in the stably stratified atmospheric boundary layer, after LES (our DATABASE64). *Solid line* is plotted after Eq. 70 with $C_u = k/R_\infty = 1.6$. *Open triangles* correspond to $\varsigma = z/L$, *black triangles* to $\varsigma = z/[(1 + C_\Omega \Omega z/E_K^{1/2})L]$ with $C_\Omega = 1$

# Comparisons

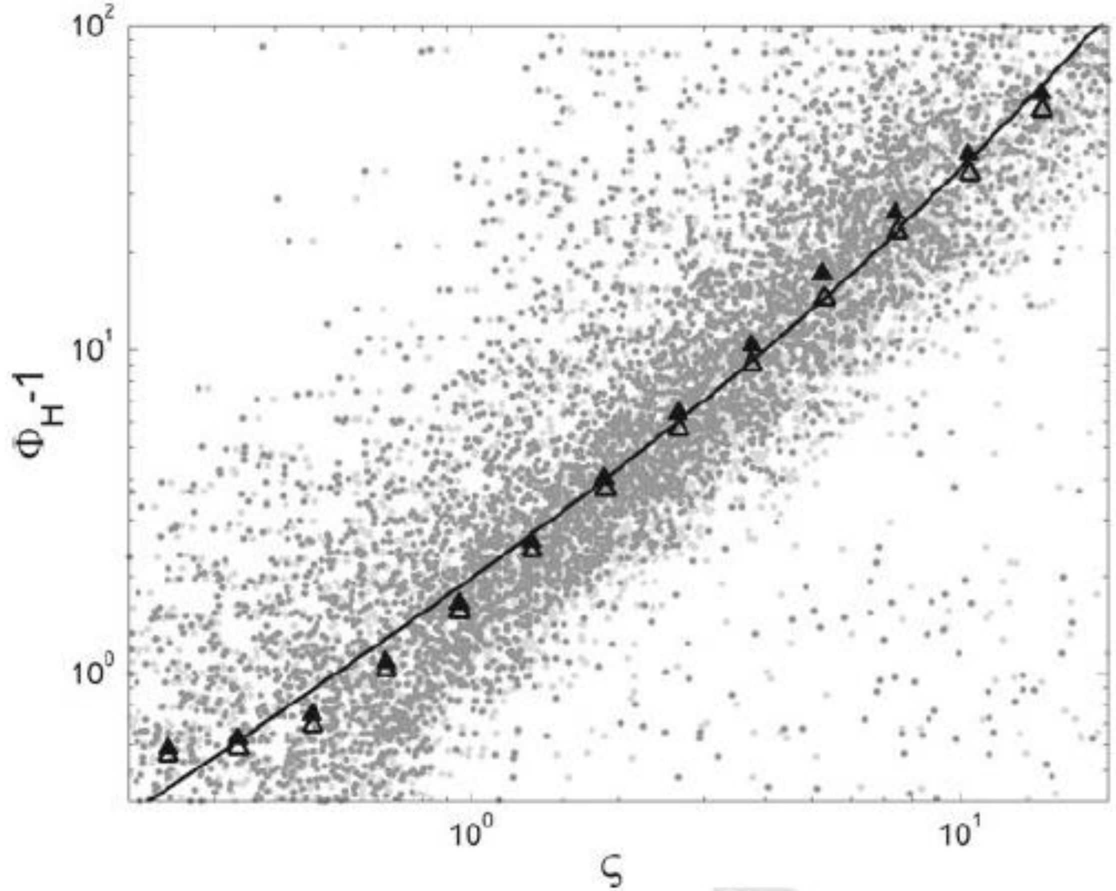


**Fig. 11** Same as in Fig. 10 but for the dimensionless potential temperature gradient $\Phi_H = (-k_T z \tau^{1/2}/F_z)(\partial\Theta/\partial z)$. *Solid line* is plotted after Eq. 86. *Open triangles* correspond to $\varsigma = z/L$, *black triangles* to $\varsigma = z/[(1 + C_\Omega \Omega z/E_K^{1/2})L]$

# Comparison with GABLS1 (Holtslag et al, 2003) Nocturnal Stable PBL

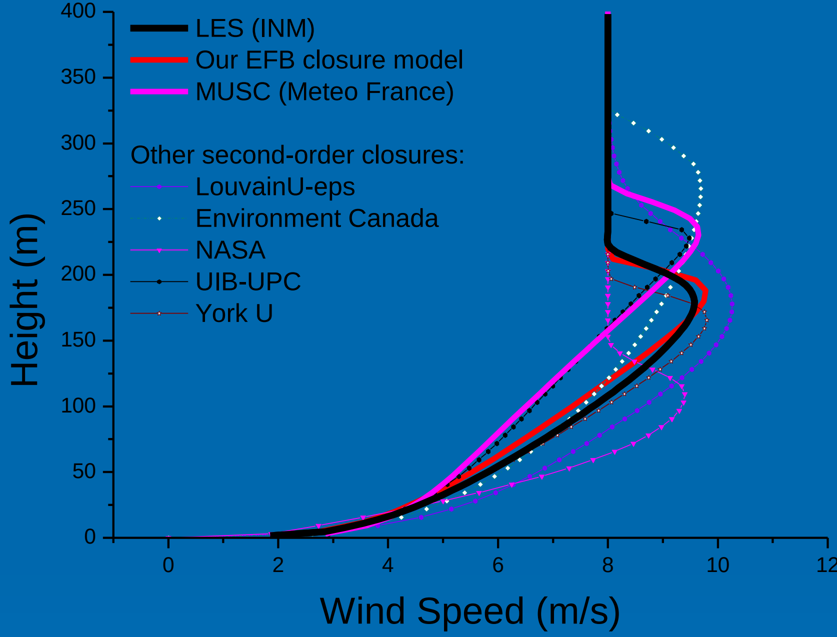


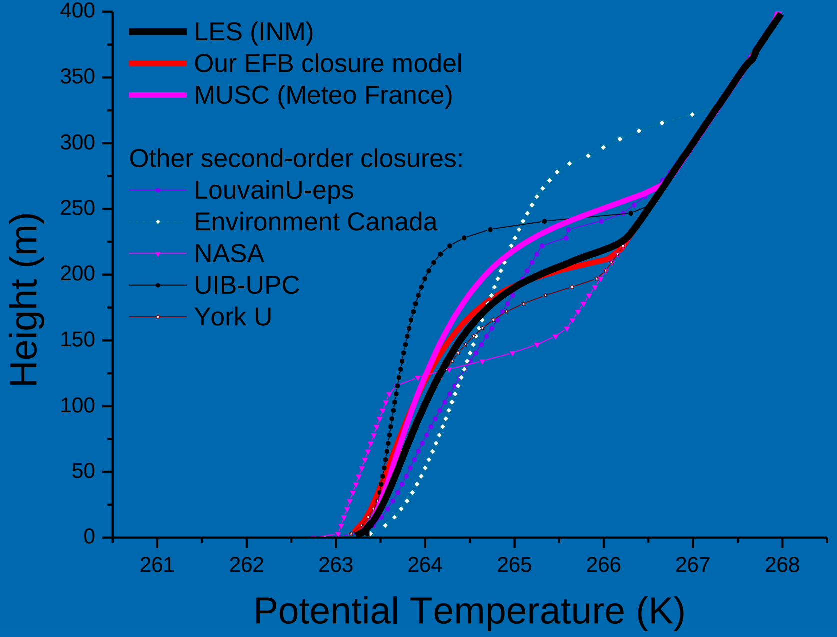


EFB-closure profiles of the wind speed and potential temperature compared with the GABLS1 LES

# Temporal development of the Obukhov length-scale and friction velocity

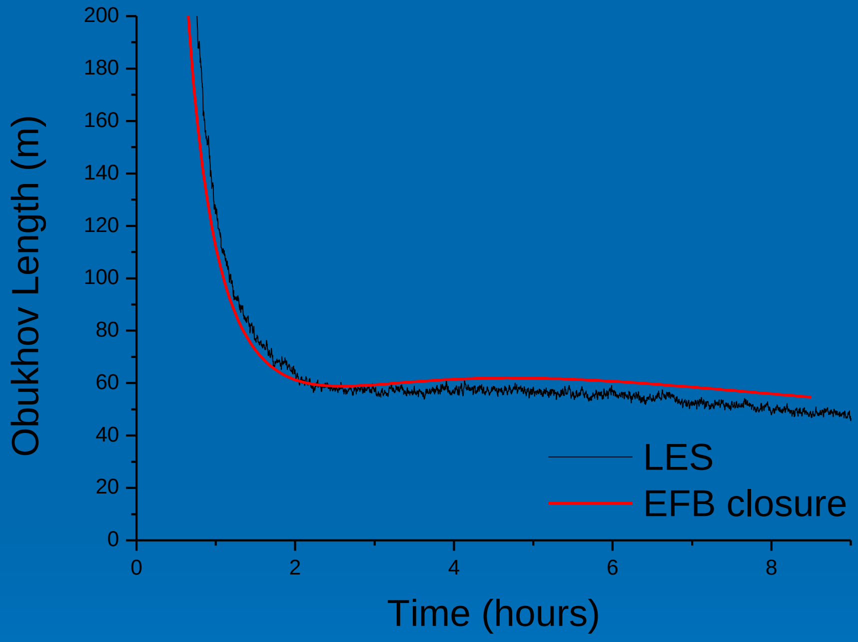


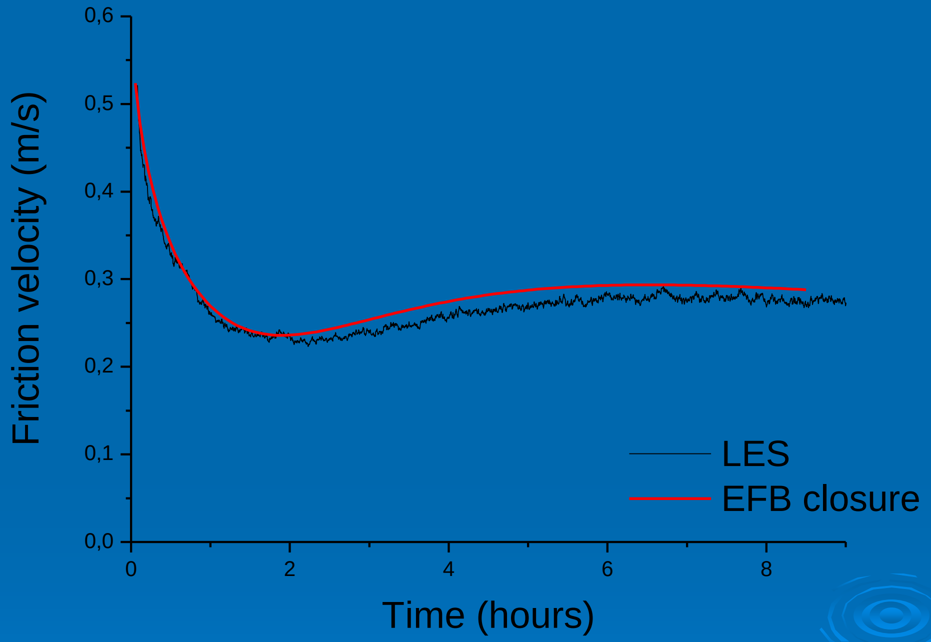


- No tuning of empirical constants to this particular case
- Very little sensitivity to spatial resolution
- Works well with only one prognostic equation (TKE)

Vertical profiles of the wind speed in Convetionally Neutral BL

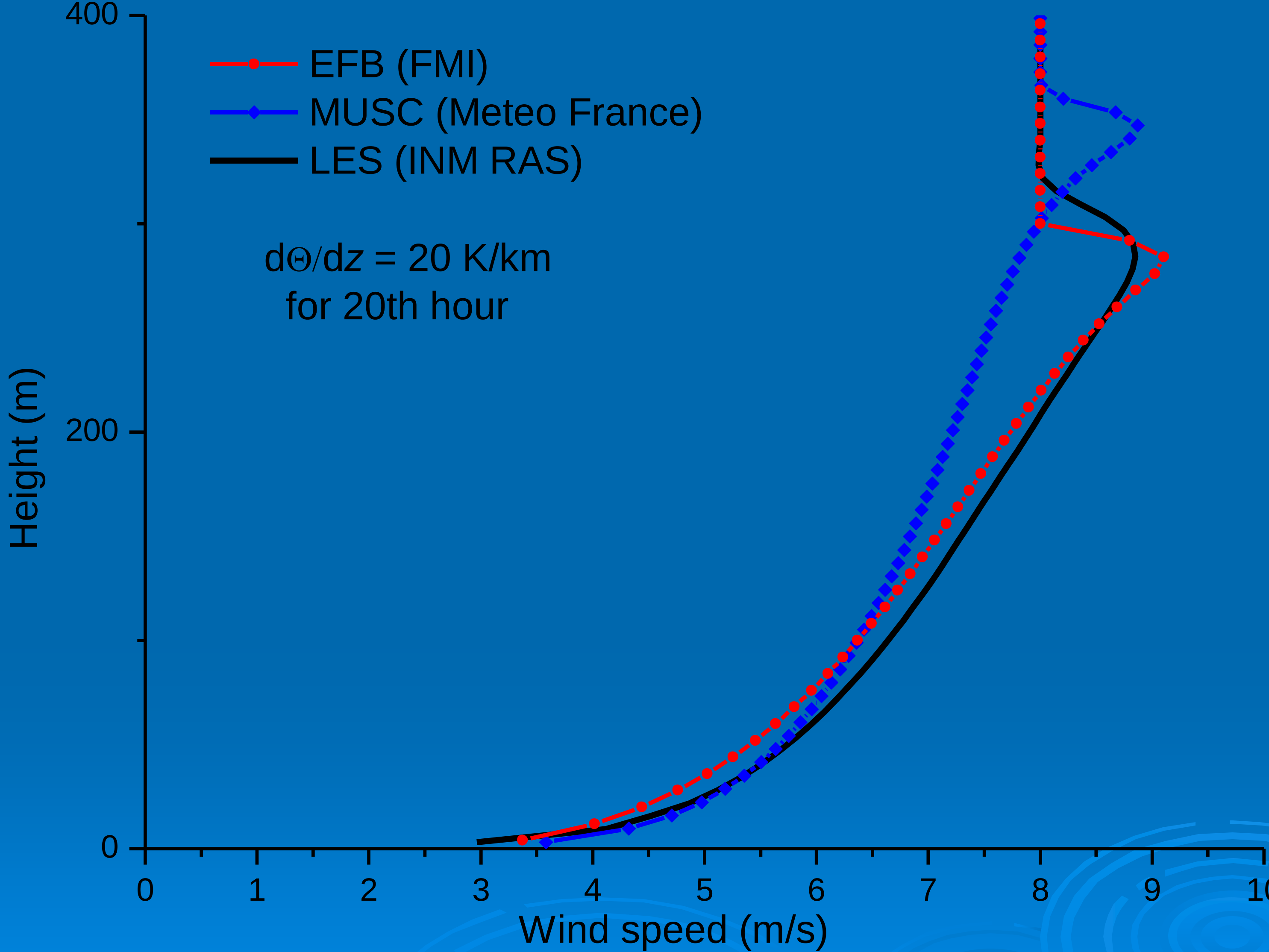

Vertical profiles of potential temperature in Convetionally Neutral BL

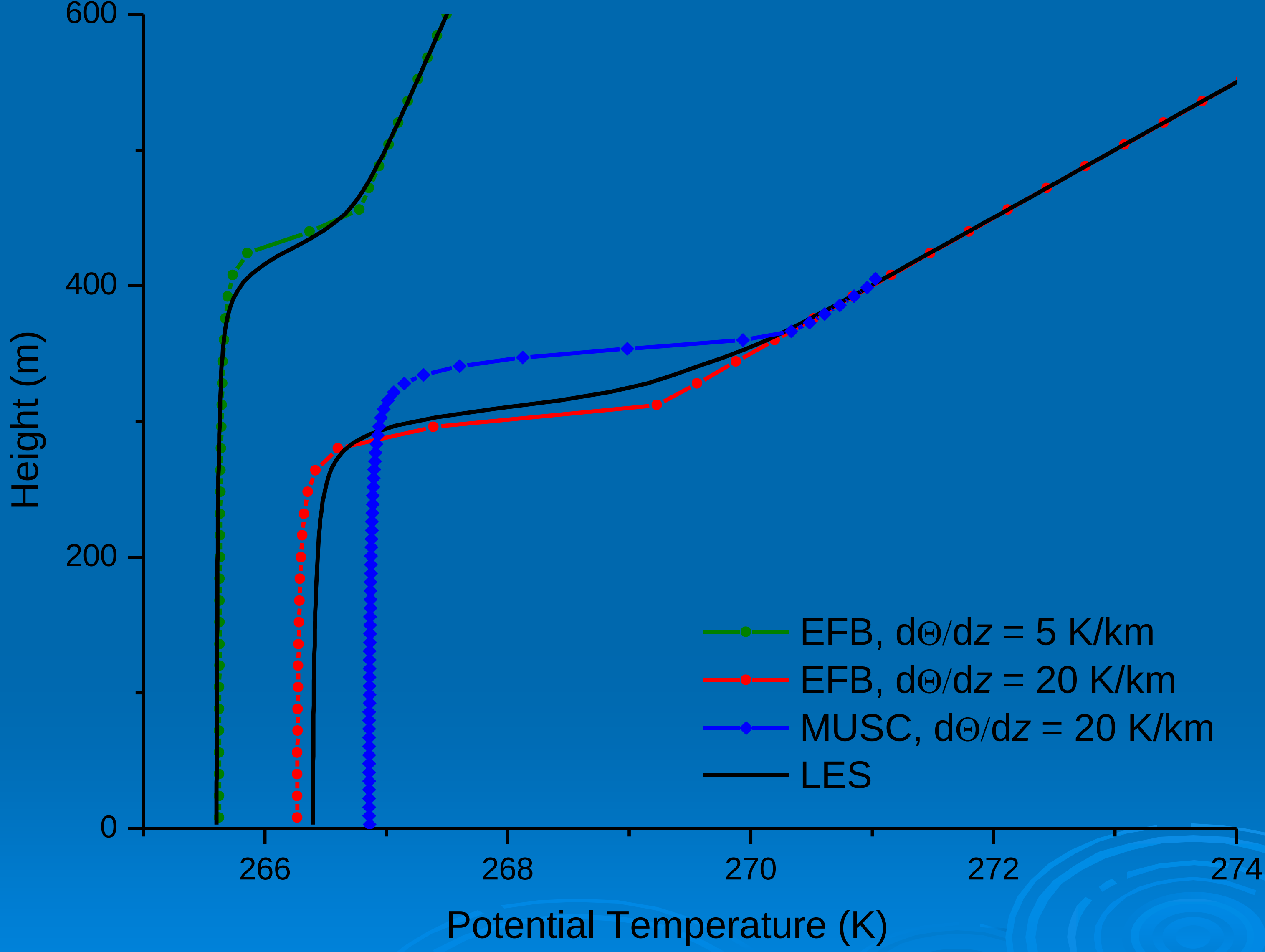

# Large-Scale Internal Gravity Waves (IGW)

**Basic Equations:**

$$\frac{\partial \mathbf{V}^W}{\partial t} = -(\mathbf{U}\cdot\nabla)\mathbf{V}^W - \nabla\left(\frac{P^W}{\rho_0}\right) + \beta\Theta^W\mathbf{e} - \left(\mathbf{V}^W\cdot\nabla\right)\mathbf{V}^W,$$

$$\frac{\partial \Theta^W}{\partial t} = -(\mathbf{U}\cdot\nabla)\Theta^W - \frac{1}{\beta}\left(\mathbf{V}^W\cdot\mathbf{e}\right)N^2 - \left(\mathbf{V}^W\cdot\nabla\right)\Theta^W,$$

**Solutions of the Linearized Equations:**

$$V_\alpha^W = -\frac{k_\alpha k_z}{k_h^2}V_0^W(\mathbf{k})\cos(\omega t - \mathbf{k}\cdot\mathbf{r}),$$

for $\alpha = 1, 2,$

$$V_3^W \equiv V_z^W = V_0^W(\mathbf{k})\cos(\omega t - \mathbf{k}\cdot\mathbf{r}),$$

$$\Theta^W = -\frac{Nk}{\beta k_h}V_0^W(\mathbf{k})\sin(\omega t - \mathbf{k}\cdot\mathbf{r})$$

**Propagation of IGW in WKB:**

$$\frac{\partial \mathbf{r}}{\partial t} = \frac{\partial \omega}{\partial \mathbf{k}},$$

$$\frac{\partial \mathbf{k}}{\partial t} = -\frac{\partial \omega}{\partial \mathbf{r}},$$

**Frequency of IGW:**

$$\omega = \frac{k_h}{k}N + \mathbf{k}\cdot\mathbf{U},$$

$$N^2 = \beta\frac{\partial\overline{\Theta}}{\partial z}$$

$\mathbf{k}_h$ =constant

$$\frac{k_h}{k(z)}N(z) + \mathbf{k}\cdot(\mathbf{U}(z) - \mathbf{U}(Z_0)) = \frac{k_h}{k_0}N(Z_0),$$

# Large-Scale Internal Gravity Waves (IGW)

- We consider the large-scale IGW with random phases whose periods and wave lengths are much larger than the turbulent time and length scales.
- We represent the total velocity as the sum of the mean-flow velocity, the turbulent velocity, and the wave-field velocity:

$$\mathbf{v} = \mathbf{U} + \mathbf{u} + \mathbf{V}^{W},$$

- We neglect the wave-wave interactions at large scales, but take into account the turbulence-wave interactions.
- We assume that the energy spectrum of the ensemble of IGW is isotropic and has the power-law form: $e_W(k_0) = (\mu - 1) E_W H^{-(\mu+1)} k_0^{-\mu},$

**where** $E_W = \int [e_W(\mathbf{k}_0)/2\pi k_0^2] d\mathbf{k}_0 = \int e_W(k_0) dk_0$

# Large-Scale Internal Gravity Waves with Random phases

$$\frac{DE_K}{Dt} + \frac{\partial \Phi_K}{\partial z} = -\tau_{i3}\frac{\partial U_i}{\partial z} + \beta F_z - \varepsilon_K - \left\langle \tau_{ij}^W \frac{\partial V_i^W}{\partial x_j} \right\rangle_W + \beta \left\langle V_z^W \, \Theta^W \right\rangle_W ,$$

$$\frac{DE_\theta}{Dt} + \frac{\partial \Phi_\theta}{\partial z} = -F_z \frac{\partial \Theta}{\partial z} - \varepsilon_\theta - \left\langle F_j^W \frac{\partial \Theta^W}{\partial x_j} \right\rangle_W ,$$

$$\frac{DF_i}{Dt} + \frac{\partial}{\partial x_j}\Phi_{ij}^{(F)} = \beta_i \left\langle \theta^2 \right\rangle + \frac{1}{\rho_0}\langle \theta \nabla_i p \rangle - \tau_{i3}\frac{\partial \Theta}{\partial z} - F_j \frac{\partial U_i}{\partial x_j} - \varepsilon_i^{(F)} - \left\langle \tau_{ij}^W \frac{\partial \Theta^W}{\partial x_j} \right\rangle_W$$

$$- \left\langle F_j^W \frac{\partial V_i^W}{\partial x_j} \right\rangle_W .$$

where

$$F_i^W \approx -C_F t_T \left( \tau_{ij} \frac{\partial \Theta^W}{\partial x_j} + \tau_{i3}^W \frac{\partial \Theta}{\partial z} + F_j \frac{\partial V_i^W}{\partial x_j} \right).$$

$$\tau_{ij}^W \approx -C_\tau t_T \left( \tau_{ik} \frac{\partial V_j^W}{\partial x_k} + \tau_{jk} \frac{\partial V_i^W}{\partial x_k} \right).$$

# Budget Equations for SBL with Large-Scale Internal Gravity Waves

$$\omega = \frac{k_h}{k} N$$

$$\frac{DE_K}{Dt} + \frac{\partial \Phi_K}{\partial z} = \Pi + \beta F_z - \frac{E_K}{t_T} + \Pi^W$$

$$\frac{DE_P}{Dt} + \frac{\partial \Phi_P}{\partial z} = -\beta F_z - \frac{E_P}{C_P t_T} + \Pi_P^W$$

$$\frac{DF_z}{Dt} + \frac{\partial \Phi_F}{\partial z} = -\left\langle u_z^2 \right\rangle \frac{\partial \bar{\Theta}}{\partial z} + 2C_\theta \beta E_\theta - \frac{F_z}{C_F t_T} + \Pi_F^W$$

$$\Pi^W = \Pi^W\left(\frac{E_W}{S^2 H^2}, \frac{N(z)}{N(z_0)}\right)$$

# Turbulent Prandtl Number vs. Ri (IG-Waves)

$$\boxed{\mathrm{Pr}_T \equiv \frac{K_M}{K_H}}$$

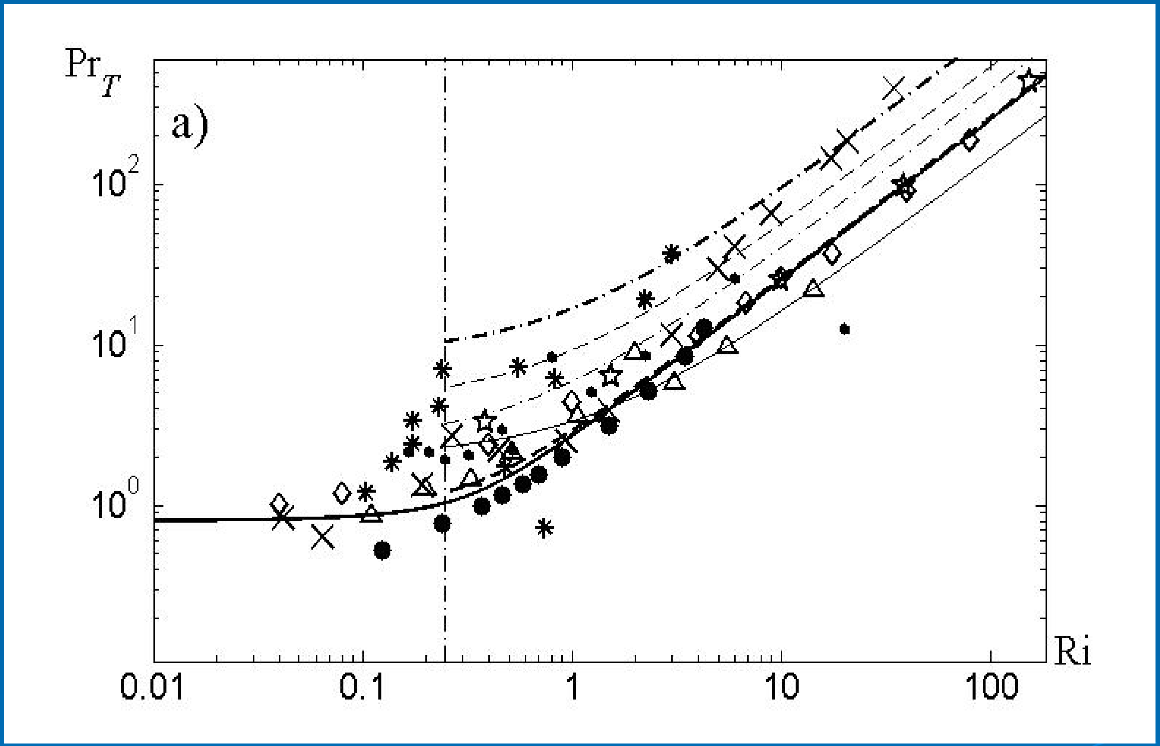


$$G \propto \frac{E^W}{S^2H^2}$$

$$Q = \frac{N^2(z)}{N^2(z_0)}$$

Meteorological observations: slanting black triangles (Kondo et al., 1978), snowflakes (Bertin et al., 1997); laboratory experiments: black circles (Strang and Fernando, 2001), slanting crosses (Rehmann and Koseff, 2004), diamonds (Ohya, 2001); LES: triangles (Zilitinkevich et al., 2008); DNS: five-pointed stars (Stretch et al., 2001). Our model with IG-waves at Q=10 and different values of parameter G: G=0.01 (thick dashed), G= 0.1 (thin dashed-dotted), G=0.15 (thin dashed), G=0.2 (thick dashed-dotted ), at Q=1 for G=1 (thin solid) and without IG-waves at G=0 (thick solid).

# $\mathrm{Ri}_f$ vs. $\mathrm{Ri}$ (IG-Waves)

$$\boxed{\mathrm{Ri}_f \equiv -\frac{\beta F_z}{\Pi}}$$

$$G \propto \frac{E^W}{S^2 H^2}$$

$$Q = \frac{N^2(z)}{N^2(z_0)}$$

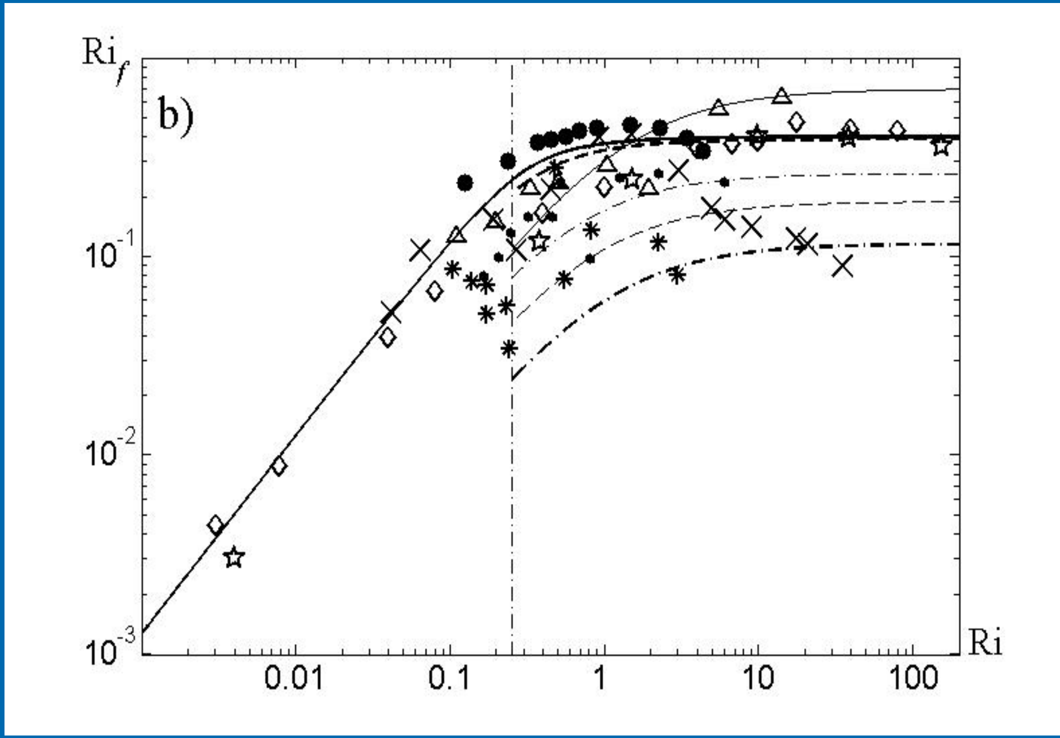


Meteorological observations: slanting black triangles (Kondo et al., 1978), snowflakes (Bertin et al., 1997); laboratory experiments: black circles (Strang and Fernando, 2001), slanting crosses (Rehmann and Koseff, 2004), diamonds (Ohya, 2001); LES: triangles (Zilitinkevich et al., 2008); DNS: five-pointed stars (Stretch et al., 2001). Our model with IG-waves at Q=10 and different values of parameter G: G=0.01 (thick dashed), G= 0.1 (thin dashed-dotted), G=0.15 (thin dashed), G=0.2 (thick dashed-dotted ), at Q=1 for G=1 (thin solid); and without IG-waves at G=0 (thick solid).

# $F_z$ vs. Ri (IG-Waves)

$$F_z = -K_H \frac{\partial \bar{\Theta}}{\partial z} + 2C_\theta \beta E_\theta t_T$$

$$G \propto \frac{E^W}{S^2 H^2}$$

$$Q = \frac{N^2(z)}{N^2(z_0)}$$

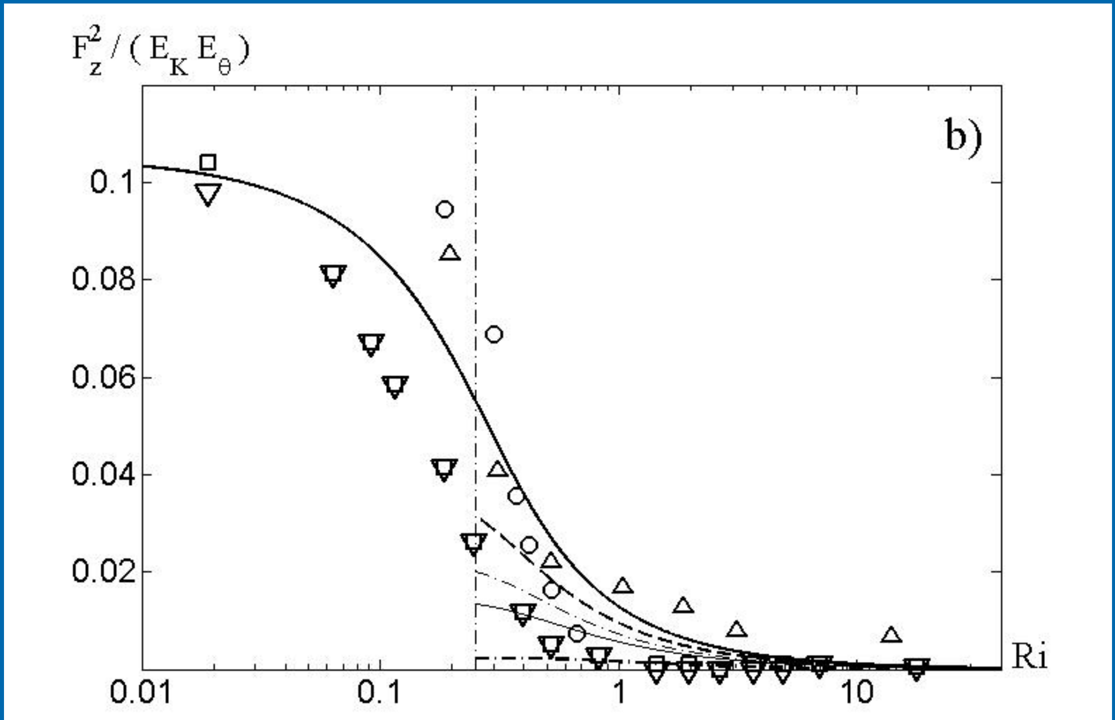


Meteorological observations: squares [CME, Mahrt and Vickers (2005)], circles [SHEBA, Uttal et al. (2002)], overturned triangles [CASES-99, Poulos et al. (2002), Banta et al. (2002)], slanting black triangles (Kondo et al., 1978), snowflakes (Bertin et al., 1997); laboratory experiments: black circles (Strang and Fernando, 2001), slanting crosses (Rehmann and Koseff, 2004), diamonds (Ohya, 2001); LES: triangles (Zilitinkevich et al., 2008); DNS: five-pointed stars (Stretch et al., 2001). Our model with IG-waves at Q=10 and different values of parameter G: G=0.001 (thin dashed), G=0.005 (thick dashed), G= 0.01 (thin dashed-dotted), G=0.05 (thick dashed-dotted), at Q=1 for G=0.1 (thin solid); and without IG-waves at G=0 (thick solid).

# $\frac{E_p}{E}$ vs. Ri (IG-Waves)

$$\boxed{E = E_K + E_p}$$

$$G \propto \frac{E^W}{S^2 H^2}$$

$$Q = \frac{N^2(z)}{N^2(z_0)}$$

$$\frac{E^W}{E} = \frac{2E_p}{E} = 0.2 - 0.8$$

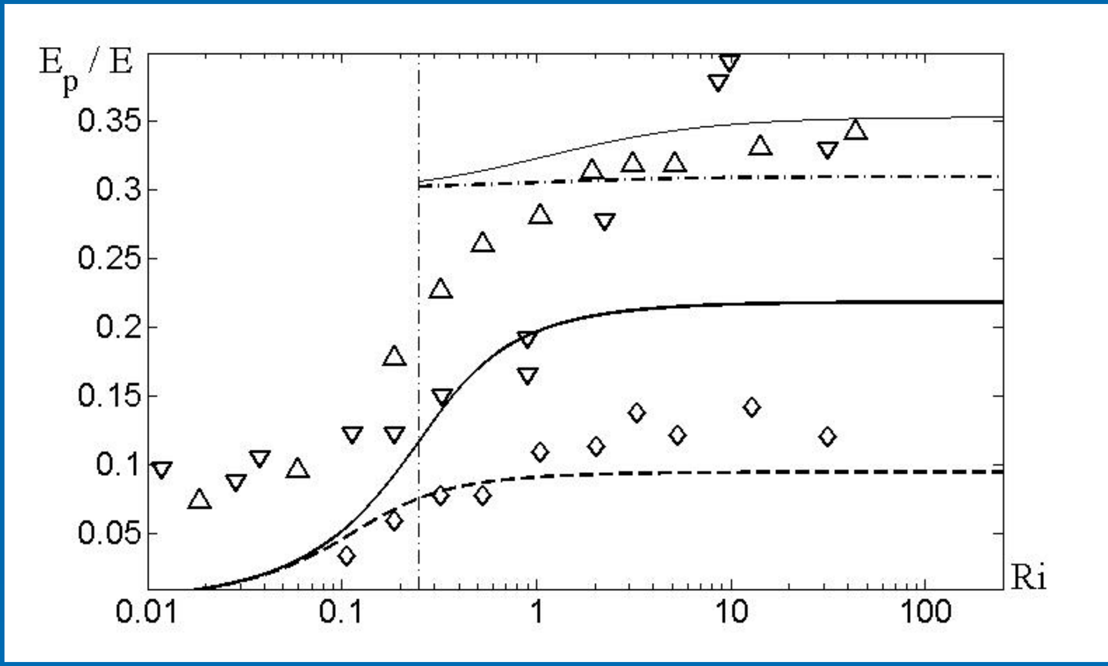


Meteorological observations: overturned triangles [CASES-99, Poulos et al. (2002), Banta et al. (2002)]; laboratory experiments: diamonds (Ohya, 2001); LES: triangles (Zilitinkevich et al., 2008). Our model with IG-waves at Q=10 and different values of parameter G: G=0.2 (thick dashed-dotted), at Q=1 for G=1 (thin solid); and without IG-waves at G=0 (thick solid for $\mathrm{Ri}_f^{\infty} = 0.4$) and (thick dashed for $\mathrm{Ri}_f^{\infty} = 0.2$).

# Large-Scale Internal Gravity Waves with Random phases

$$\frac{DE_K}{Dt} + \frac{\partial \Phi_K}{\partial z} = -\tau_{i3}\frac{\partial U_i}{\partial z} + \beta F_z - \varepsilon_K - \left\langle \tau_{ij}^W \frac{\partial V_i^W}{\partial x_j} \right\rangle_W + \beta \left\langle V_z^W \, \Theta^W \right\rangle_W ,$$

$$\frac{DE_\theta}{Dt} + \frac{\partial \Phi_\theta}{\partial z} = -F_z \frac{\partial \Theta}{\partial z} - \varepsilon_\theta - \left\langle F_j^W \frac{\partial \Theta^W}{\partial x_j} \right\rangle_W ,$$

$$\frac{DF_i}{Dt} + \frac{\partial}{\partial x_j}\Phi_{ij}^{(F)} = \beta_i \left\langle \theta^2 \right\rangle + \frac{1}{\rho_0}\left\langle \theta \nabla_i p \right\rangle - \tau_{i3}\frac{\partial \Theta}{\partial z} - F_j \frac{\partial U_i}{\partial x_j} - \varepsilon_i^{(F)} - \left\langle \tau_{ij}^W \frac{\partial \Theta^W}{\partial x_j} \right\rangle_W$$
$$- \left\langle F_j^W \frac{\partial V_i^W}{\partial x_j} \right\rangle_W .$$

**where**

$$F_i^W \approx -C_F t_T \left( \tau_{ij} \frac{\partial \Theta^W}{\partial x_j} + \tau_{i3}^W \frac{\partial \Theta}{\partial z} + F_j \frac{\partial V_i^W}{\partial x_j} \right).$$

$$\tau_{ij}^W \approx -C_\tau t_T \left( \tau_{ik} \frac{\partial V_j^W}{\partial x_k} + \tau_{jk} \frac{\partial V_i^W}{\partial x_k} \right).$$

# Budget Equations for IGW: S=0

$$\frac{DE_K^W}{Dt} + \operatorname{div}\boldsymbol{\Phi}^W = \left\langle \tau_{ij}^W \frac{\partial V_i^W}{\partial x_j} \right\rangle_W ,$$

$$\frac{DE_P^W}{Dt} = \frac{\beta^2}{N^2} \left\langle F_j^W \frac{\partial \Theta^W}{\partial x_j} \right\rangle_W ,$$

**where**

$$\tau_{ij}^W \approx -C_\tau t_T \left( \tau_{ik} \frac{\partial V_j^W}{\partial x_k} + \tau_{jk} \frac{\partial V_i^W}{\partial x_k} \right).$$

$$F_i^W \approx -C_F t_T \left( \tau_{ij} \frac{\partial \Theta^W}{\partial x_j} + \tau_{i3}^W \frac{\partial \Theta}{\partial z} + F_j \frac{\partial V_i^W}{\partial x_j} \right).$$

$$\boldsymbol{\Phi}^W = \frac{1}{\rho_0} \left\langle p^W \mathbf{V}^W \right\rangle_W = \int \mathbf{C}_g(\mathbf{k}) \widetilde{E}^W(\mathbf{k})\, d\mathbf{k} ,$$

**Total wave energy:**

$$E^W = E_K^W + E_p^W ,$$

$$\frac{DE^W}{Dt} + \frac{\partial}{\partial z}\left[ V_g(Q) E^W \right] = -\gamma_d(E^W) E^W$$

**where**

$$\gamma_d(E^W) = C_F (1 + \Pr_0) \pi^W \frac{\ell_T}{H^2} \sqrt{E_K(E^W)}$$

$$V_g(Q) = \frac{\mu - 1}{\mu} N_0 H f(Q)$$

# Wave Richardson Number

$$\mathrm{Ri}_W = \frac{N_0^2 H^2}{E_W \, \mathrm{Pr}_T^{(0)} \, \Gamma}$$

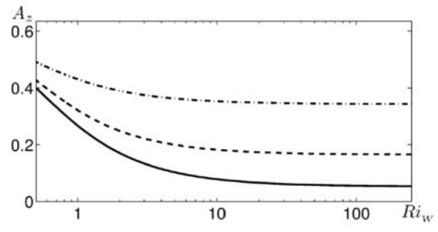


**Figure 1.** The anisotropy parameter $A_z$ versus the parameter for different values of the parameter $C_0$: $C_0 = 1/15$ (solid), $C_0 = 0.1$ (dashed), $C_0 = 0.217$ (dashed-doted).

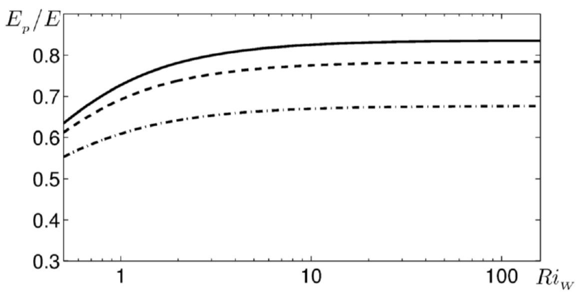


**Figure 2.** The ratio of potential to the total energy versus the parameter $\mathrm{Ri}_W$.

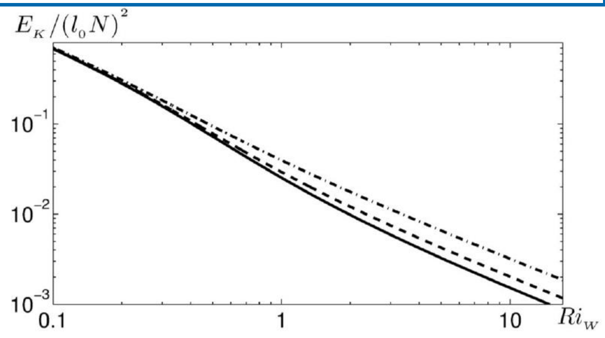


**Figure 3.** Kinetic energy (in Ozmidov units) versus the parameter $\mathrm{Ri}_W$.

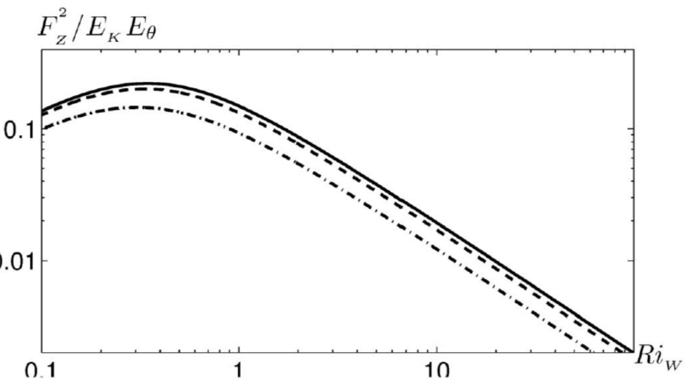


**Figure 4.** The non-dimensional squared potential temperature flux versus the parameter $\mathrm{Ri}_W$.

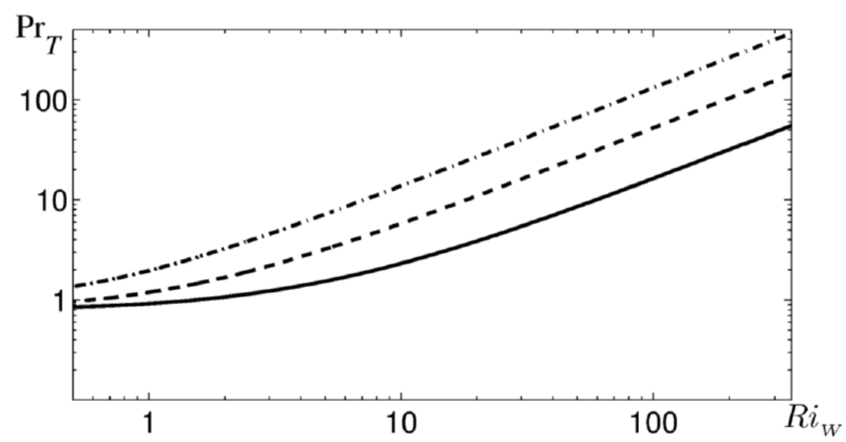


**Figure 5.** The turbulent Prandtl number $\mathrm{Pr}_T$ versus the parameter $\mathrm{Ri}_W$.

# Spatial Profiles

$$H_{eff} = H \frac{\mu - 1}{2\mu\Gamma\sqrt{2C_F^3/3}\,(1+\Pr_0)}\left(\frac{H}{\ell_T}\right)^2$$

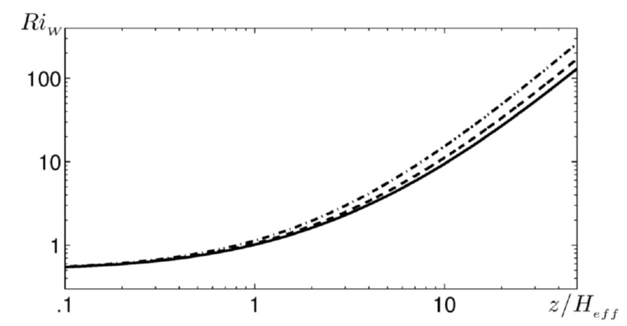


**Figure 7.** The vertical profile of the parameter $\mathrm{Ri}_W(z)$.

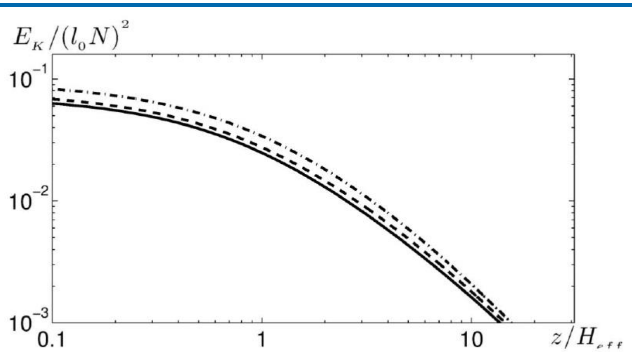


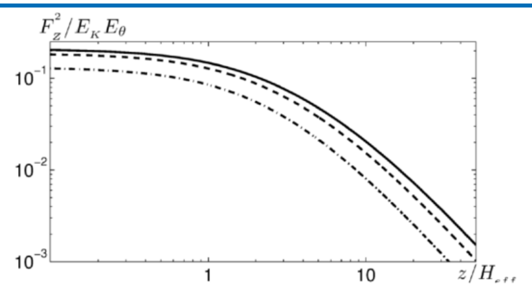


**Figure 9.** The vertical profile of the non-dimensional squared flux of the potential temperature.

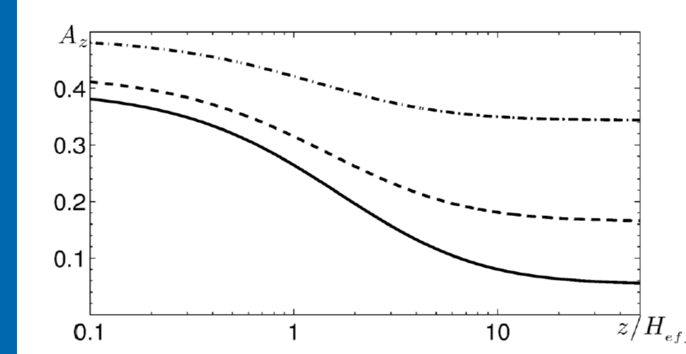


**Figure 10.** The vertical profile of the anisotropy parameter $A_z$.

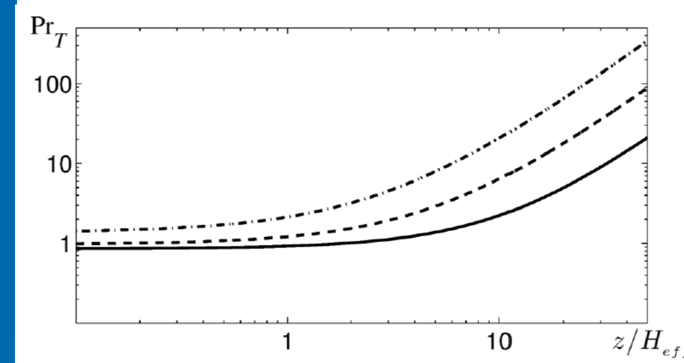


**Figure 11.** The vertical profile of the turbulent Prandtl number, $\Pr_T$.

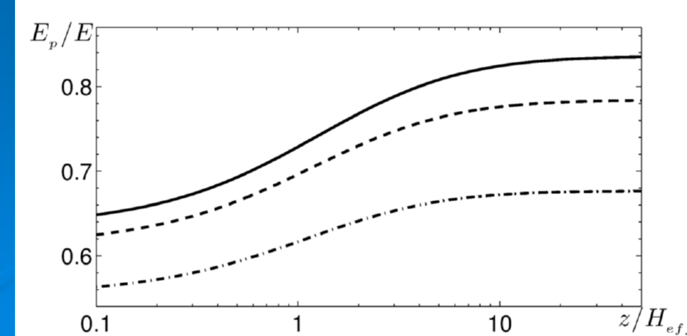


**Figure 12.** The vertical profile of the ratio of the potential to the total energy.

# Laboratory Experiments of Stably Stratified Turbulent Flow

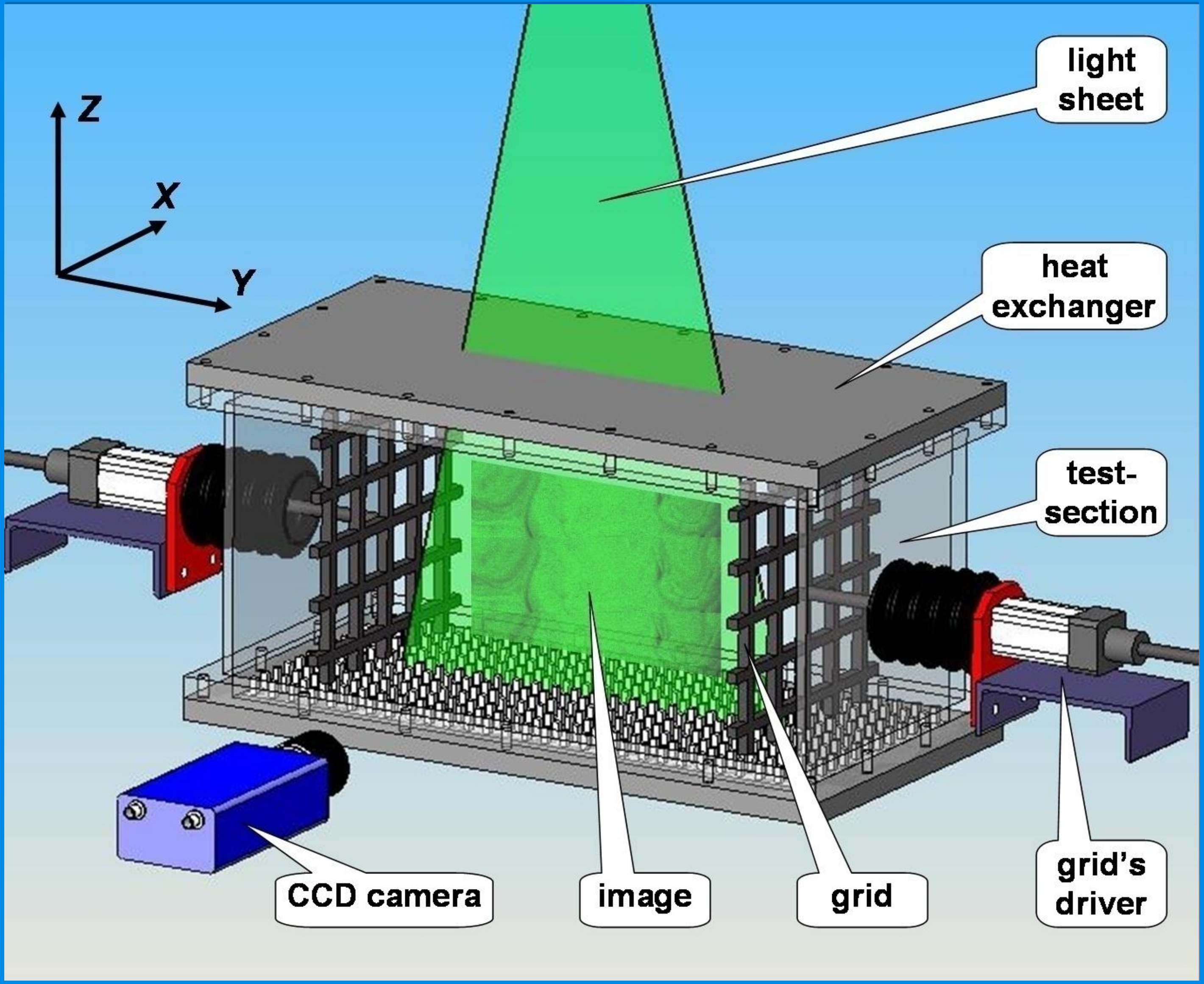

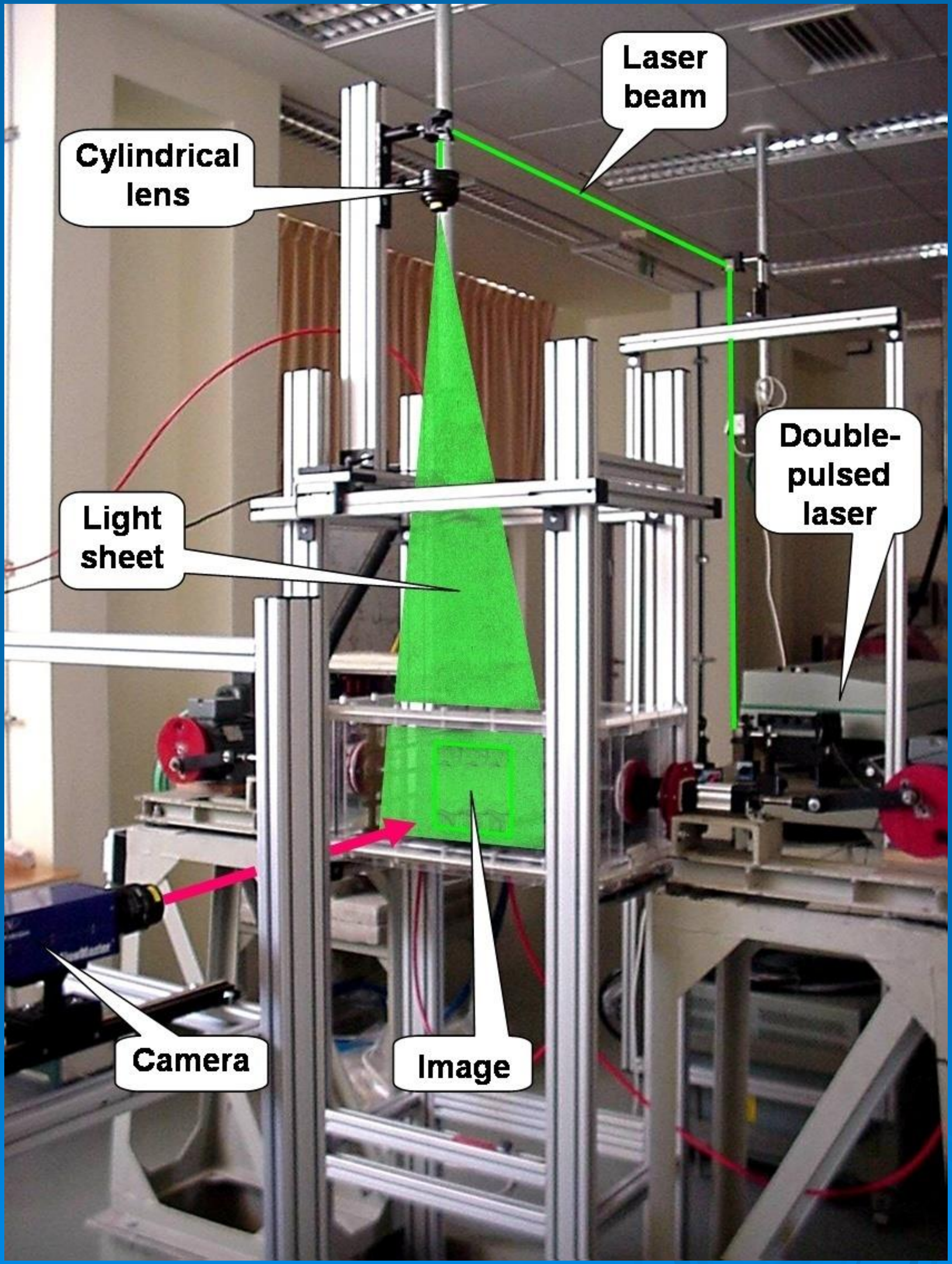


**Experimental set - up: oscillating grids turbulence generator and particle image velocimetry system**

# Particle Image Velocimetry System

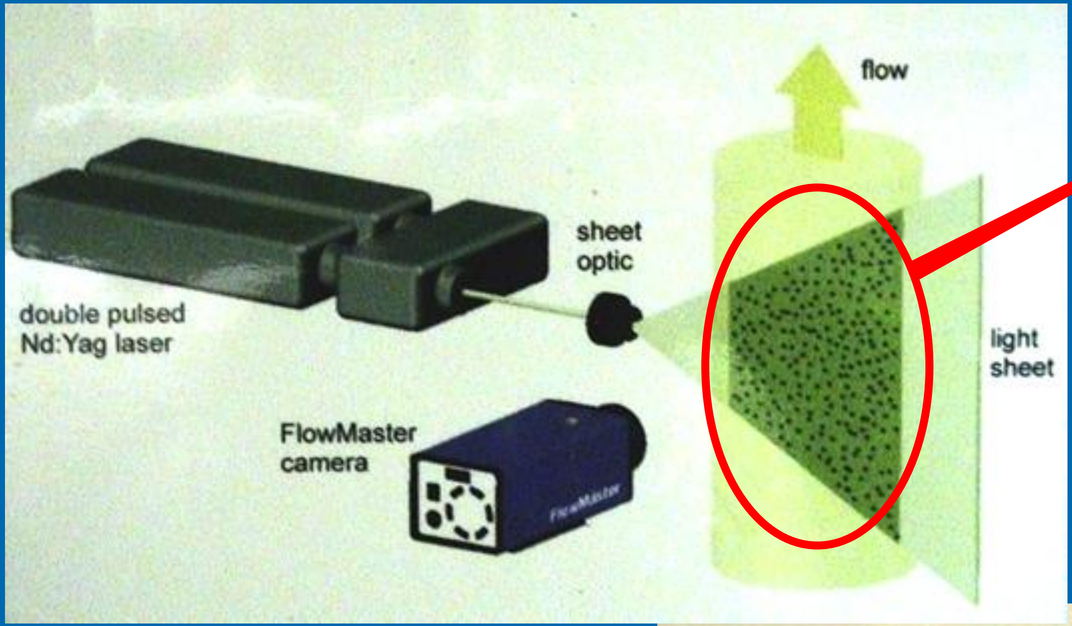


Raw image of the incense smoke tracer particles in oscillating grids turbulence

## Particle Image Velocimetry Data Processing

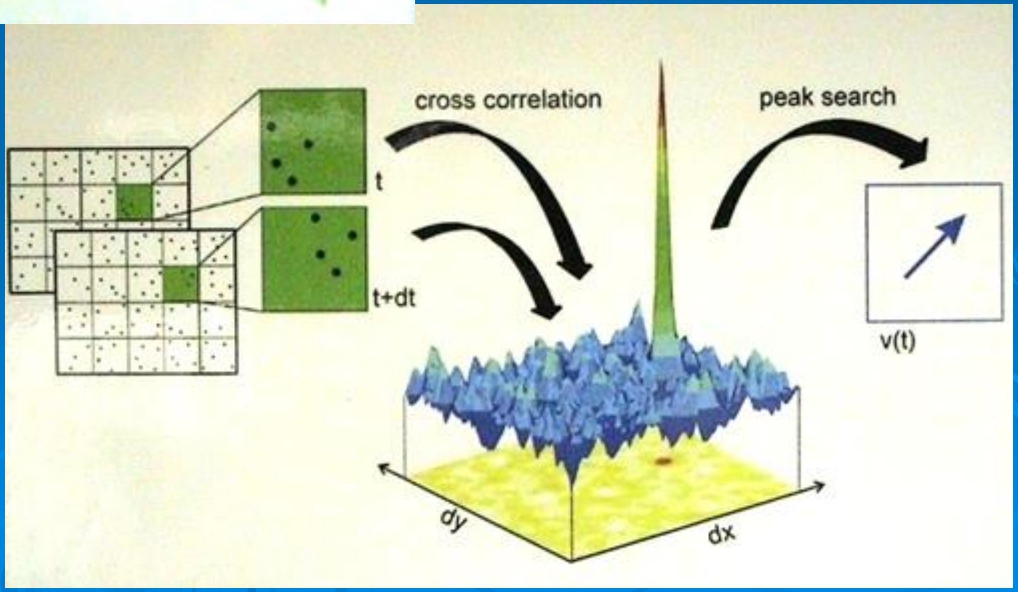

# Instantaneous Streamlines of the Flow and Velocity Fluctuations

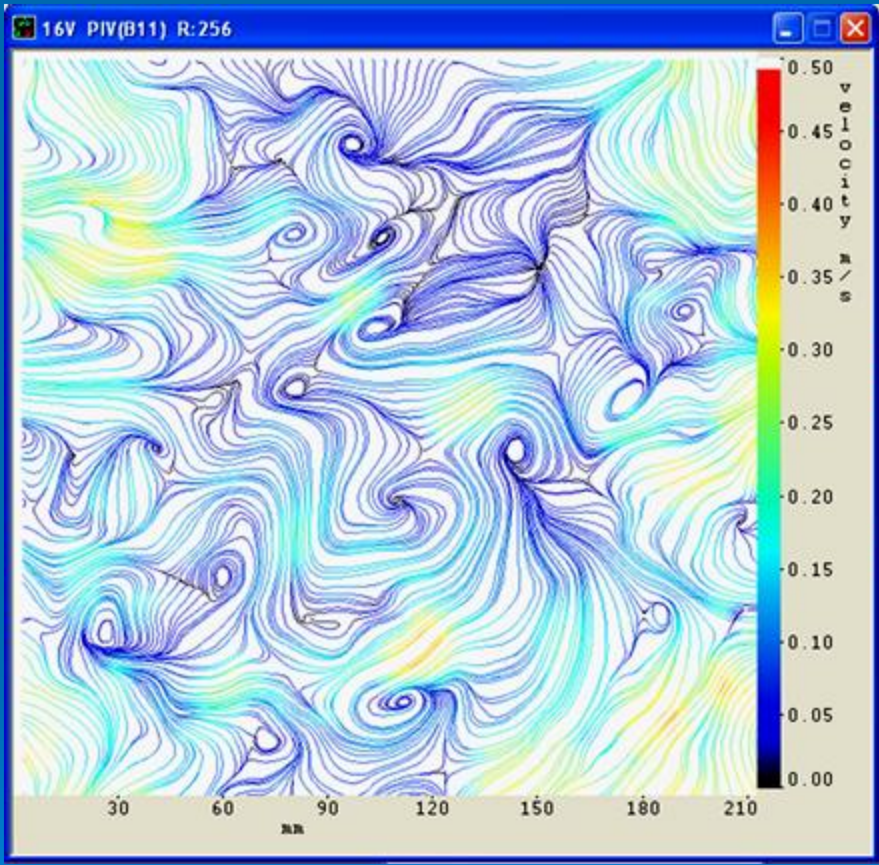


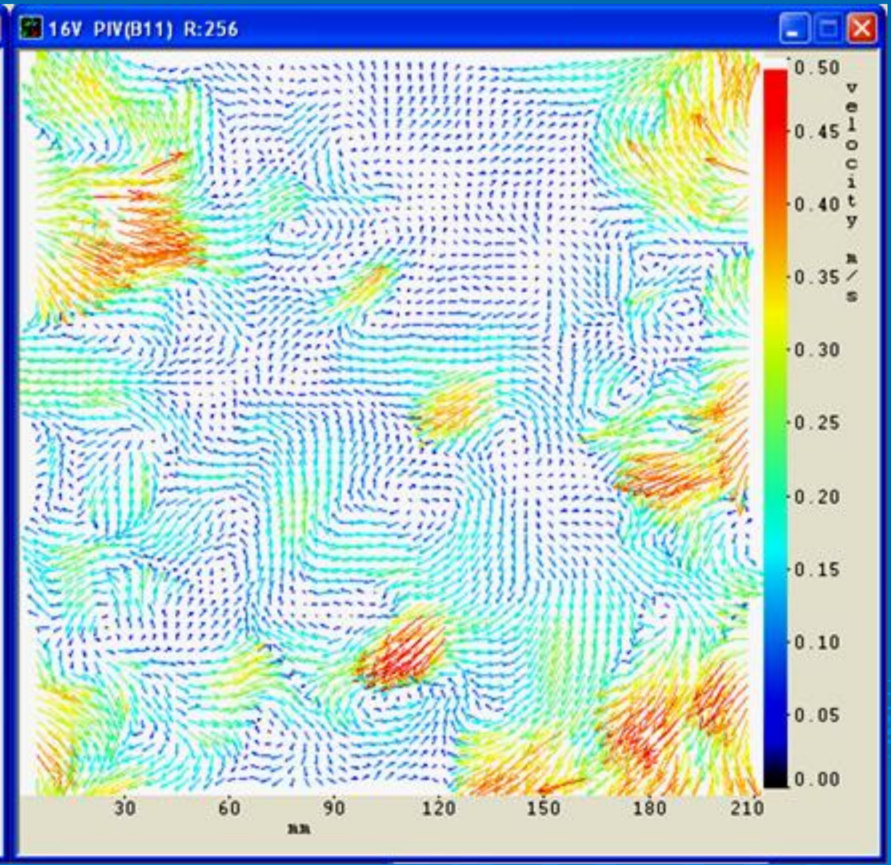

# Turbulent Energy Spectrum

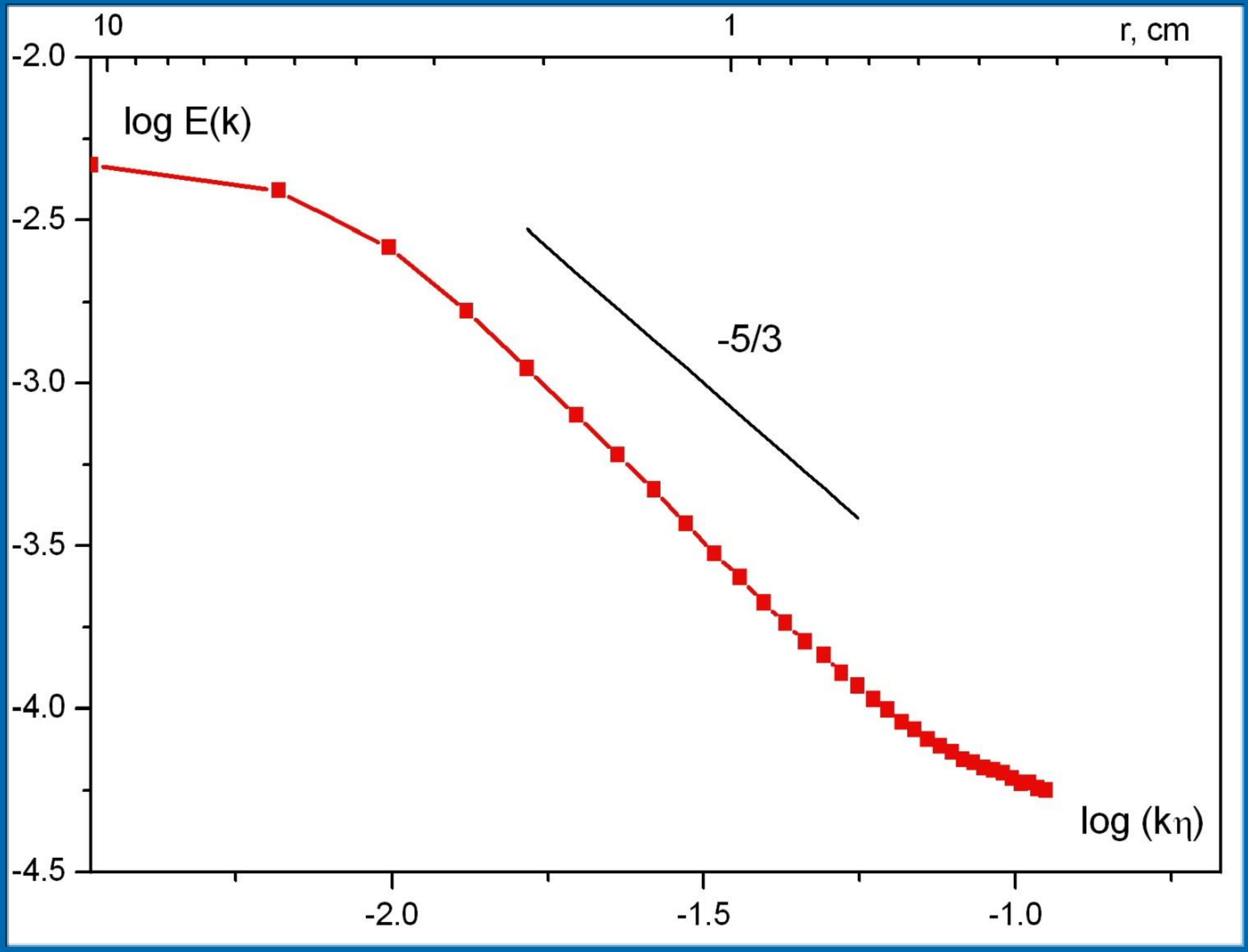

## ➢ Stably stratified turbulent flows

A fog-ridden, pooled shallow SBL in a mountain valley

(SBL- stable  boundary layer)

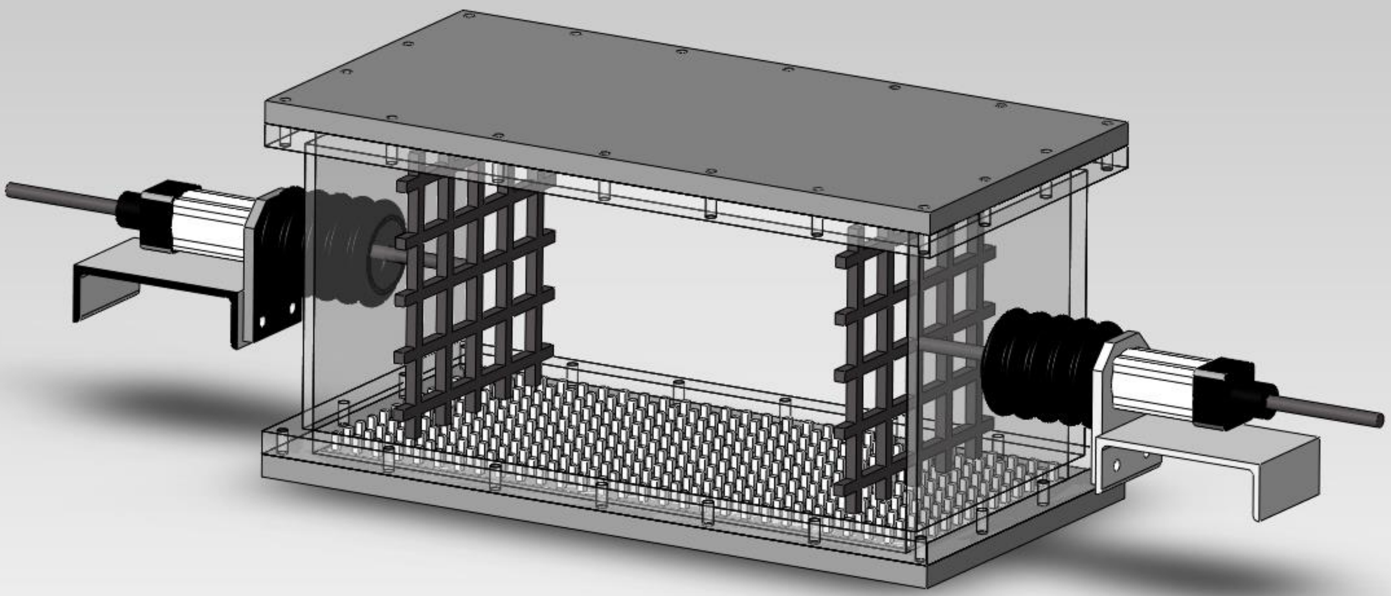

# Experim 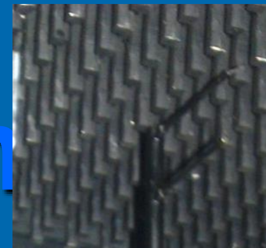 l Setup

**Unstably stratified**

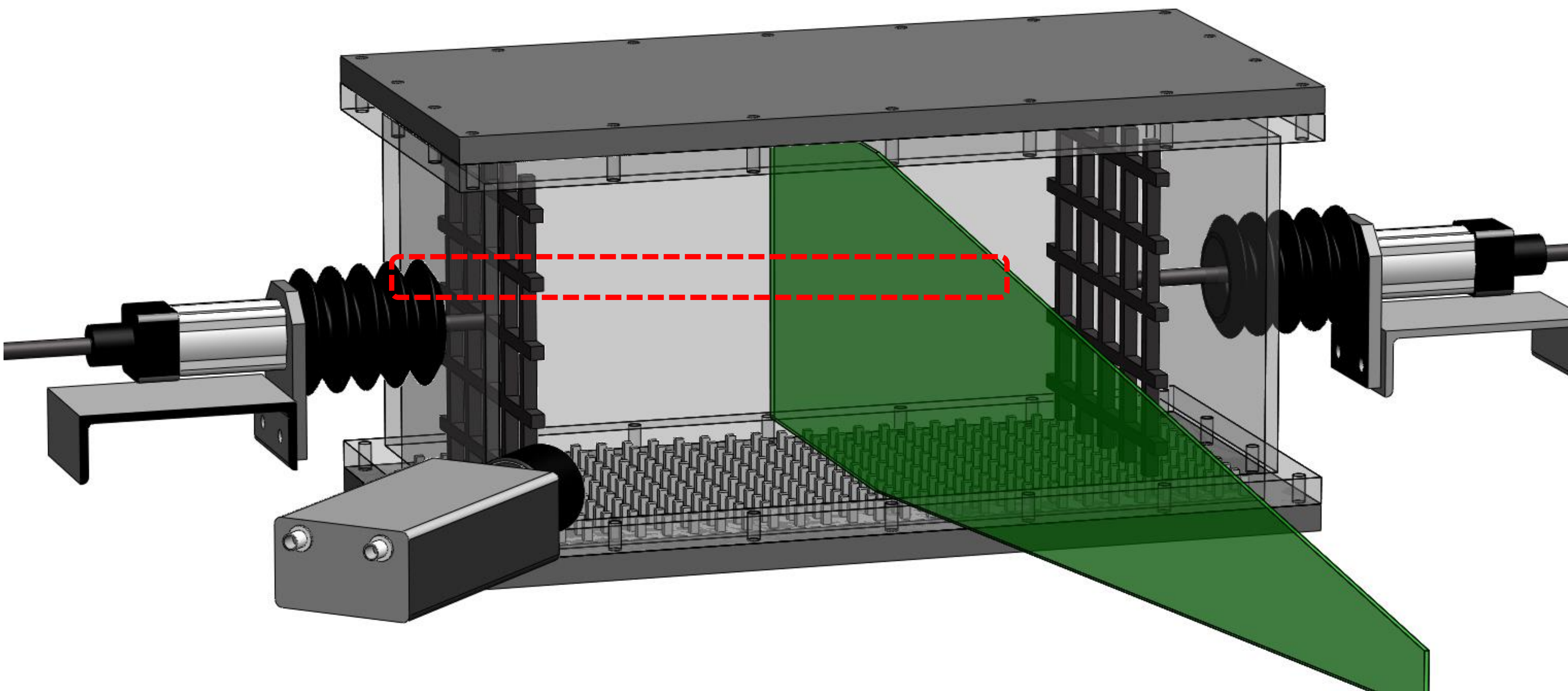

# Budget Equations for SBL

- Turbulent kinetic energy: $E_K = \frac{1}{2}\langle \mathbf{u}^2 \rangle$
- Potential temperature fluctuations: $E_\theta = \frac{1}{2}\langle \theta^2 \rangle$
- Flux of potential temperature : $\mathbf{F} = \langle \mathbf{u}\ \theta \rangle$

$$\frac{DE_K}{Dt} + \operatorname{div}(\mathbf{\Phi}_u) - \Pi - \beta F_z = -D_K$$

$$\frac{DE_\theta}{Dt} + \operatorname{div}(\mathbf{\Phi}_\theta) + \frac{N^2}{\beta} F_z = -D_\theta$$

$$\frac{DF_i}{Dt} + \operatorname{div}_j(\Phi_{ij}^F) + (\mathbf{F}\cdot\nabla)\overline{U}_i + \frac{N^2}{\beta}\tau_{ij} e_j - 2C_\theta \beta e_i E_\theta = -D_i^F$$

$$C_\theta \beta_i \langle \theta^2 \rangle = \beta_i \langle \theta^2 \rangle + \frac{1}{\rho_0}\langle \theta \nabla_i p \rangle$$

$$D_K = \frac{E_K}{t_T} \qquad D_\theta = \frac{E_\theta}{C_\theta t_T} \qquad D_i^F = \frac{F_i}{C_F t_T}$$

$$\Pi = -\tau_{ij} \nabla_j \overline{U}_i \boxed{+ \langle \mathbf{u}\cdot\mathbf{f}_f \rangle}$$

# Theoretical Analysis

## The energy- and flux-budget turbulence closure (EFB model)

$$(\ell_*\nabla_*T)^2 = \left[(\ell_x\nabla_x T)^2 + (\ell_y\nabla_y T)^2 + (\ell_z\nabla_z T)^2\right]\cdot\left[1 + 2C_\theta C_F \beta\tau_0^2 (\nabla_z T)\right]^{-1}$$

TKE

$$E_k = \langle u_i u_i \rangle / 2$$

TTE
=TKE+TPE

$$E_\theta = \langle \theta^2 \rangle / 2$$

TPE

$$E_p = \left(\beta^2 / N^2\right) E_\theta$$

$$\beta = g/T_0$$

$$N^2 = \beta\nabla_z T$$

Turbulent
heat flux

$$F_i = \langle u_i \theta \rangle$$

$$\mathrm{steady-state}$$

$$\tau_x \approx \tau_y \approx \tau_z = \tau_0$$

$$o[\ell^3 / L_T^3; \ell^3 / (L_T^2 L_U)] << 1$$

$$\varepsilon_\theta = \langle \theta^2 \rangle / 2\tau_0$$

$$\varepsilon_i^{(F)} = F_i / C_F \tau_0$$

$$\langle u_i u_i \rangle >> \langle u_i u_j \rangle_{i \neq j}$$

$$\boxed{\frac{(\ell_*\nabla_*T)^2}{\langle \theta^2 \rangle} = \frac{1}{2C_F} = const}$$

$$E_z = \langle \boldsymbol{u}_z^2 \rangle / 2$$

$$-\langle u_i u_j \rangle \nabla_j U_i << \langle \boldsymbol{u} \cdot \boldsymbol{f}_f \rangle$$

$$\underbrace{\sqrt{\langle u_z^2 \rangle}}_{u_z^{rms}} = \underbrace{\left[\left\langle (u_z^*)^2 \right\rangle - C_u \ell_z \beta \sqrt{\langle \theta^2 \rangle}\right]^{1/2}}_{\tilde{u}_z}$$

$$\langle (u_z^*)^2 \rangle = 2\tau \langle u_z f_z \rangle / [1 + C_r(1 - 1/3Az)]$$

$$A_z = E_z / E_k$$

# Comparison of Experimental and Theoretical Results

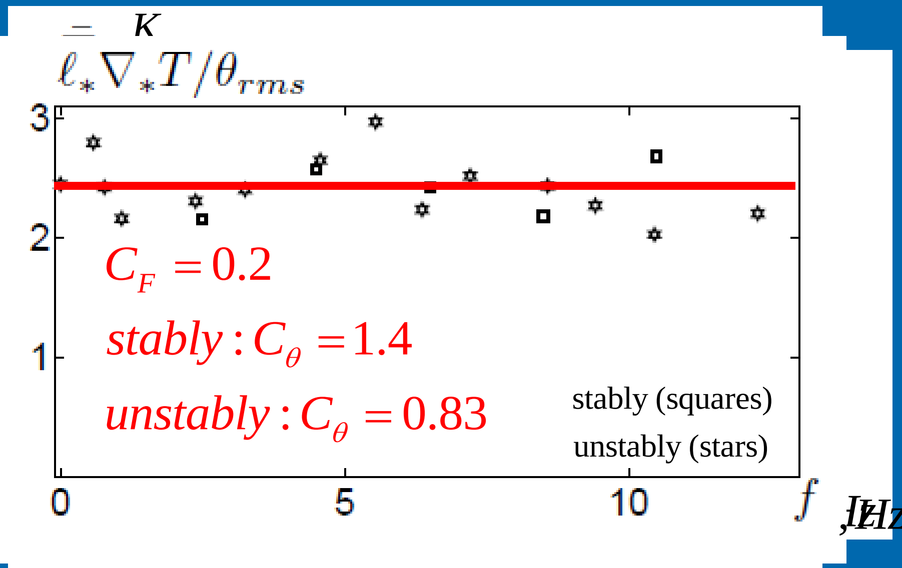


$$\boxed{\frac{\left(\ell_* \nabla_* T\right)^2}{\theta_{rms}^2} = \frac{1}{2C_F} = const}$$

$$\left(\ell_* \nabla_* T\right)^2 = \frac{\left(\ell_x \nabla_x T\right)^2 + \left(\ell_y \nabla_y T\right)^2 + \left(\ell_z \nabla_z T\right)^2}{1 + 2 C_\theta C_F \beta \tau_0^2 \left(\nabla_z T\right)}$$

$$\theta_{rms} = \sqrt{\left\langle \theta^2 \right\rangle}$$

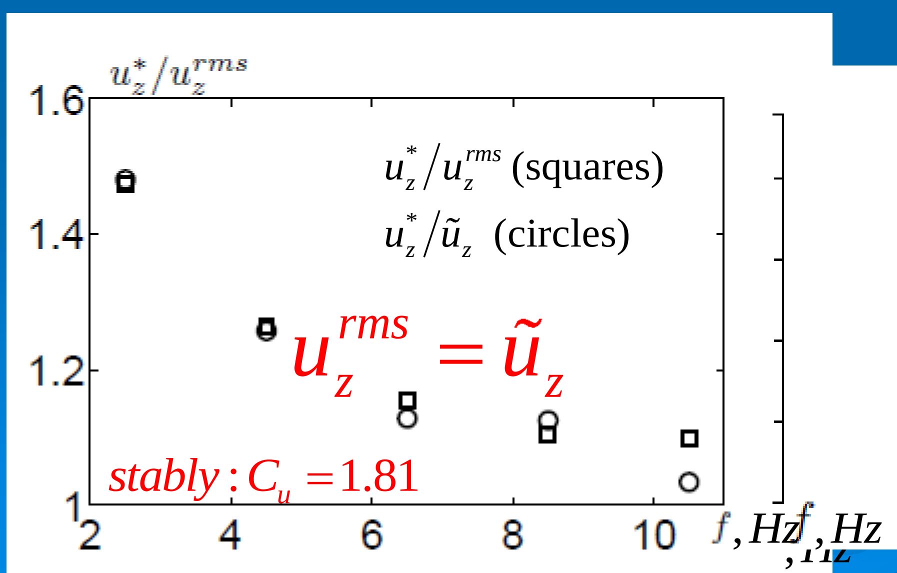


$$\tilde{u}_z = \left[ \left\langle \left(u_z^*\right)^2 \right\rangle - C_u \ell_z \beta \sqrt{\left\langle \theta^2 \right\rangle} \right]^{1/2}$$

$$\left\langle (u_z^*)^2 \right\rangle = 2\tau \left\langle u_z f_z \right\rangle / [1 + C_r (1 - 1/3Az)]$$

$$u_z^{rms} = \sqrt{\left\langle u_z^2 \right\rangle}$$

# Turbulent Richardson number

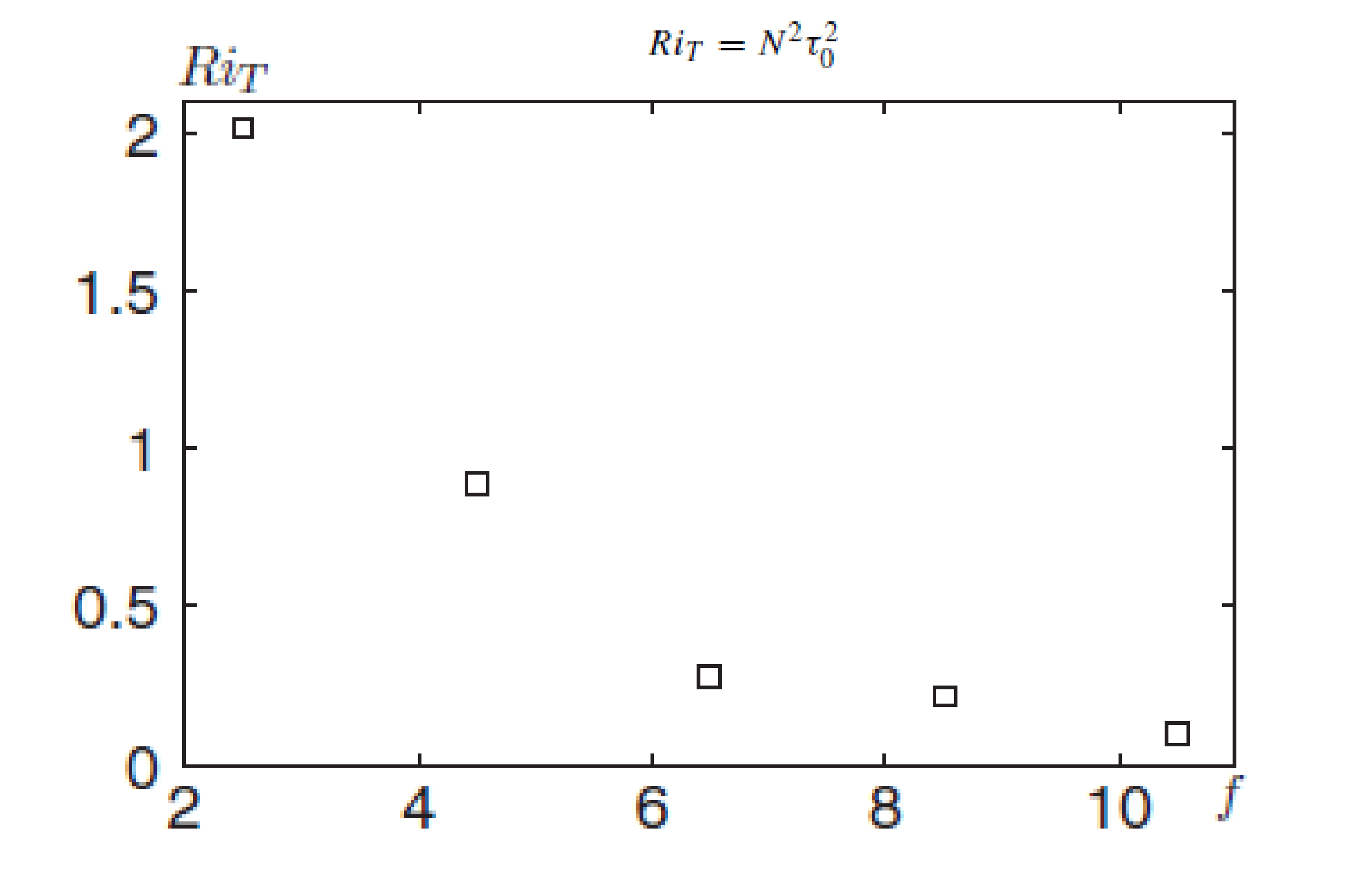

# Experimental Set-up with Sheared Temperature Stratified Turbulence

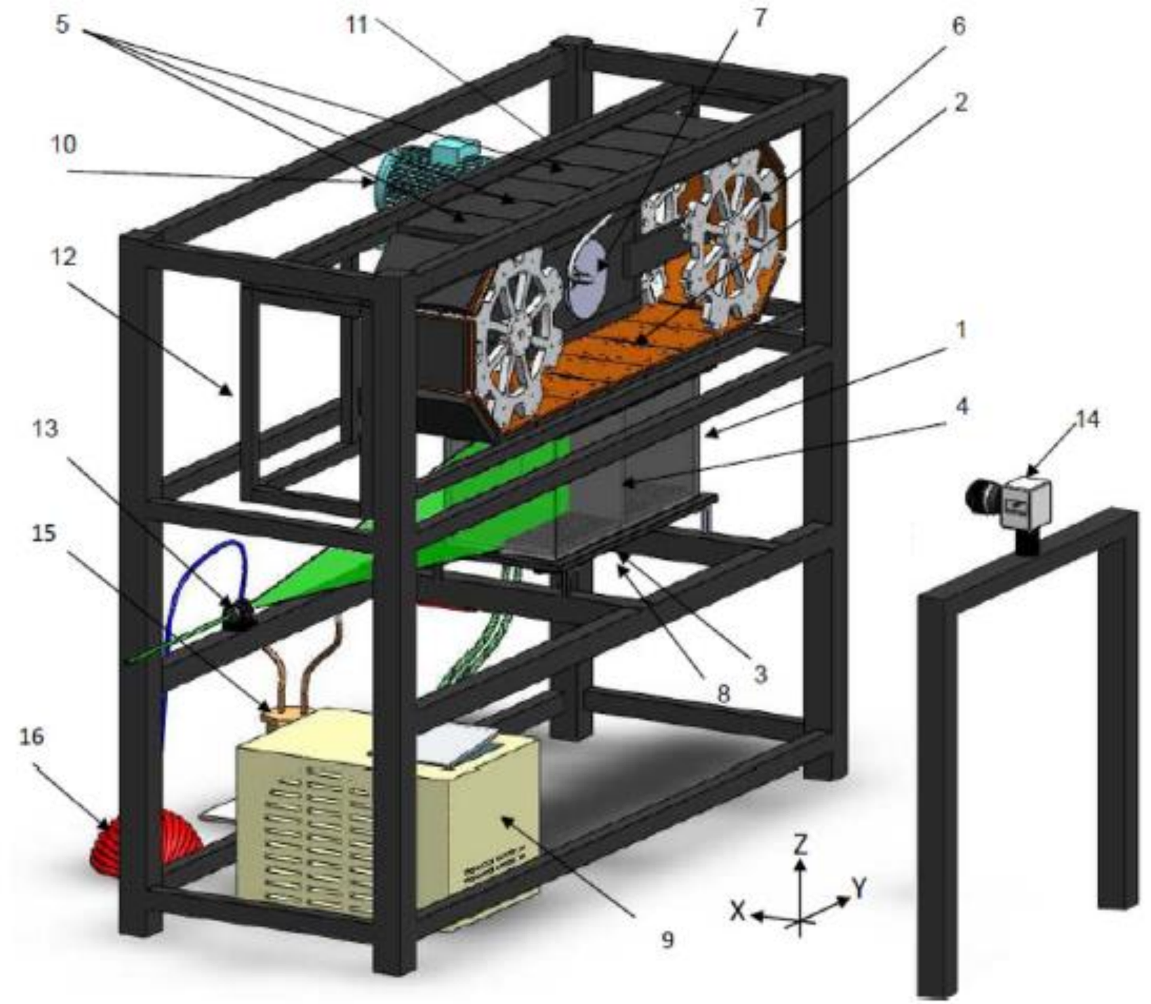


FIG. 1. Scheme of the experimental set-up with sheared temperature stratified turbulence: 1—rectangular cavity; 2—heated top wall; 3—cooled bottom wall; 4—internal partition; 5—plate heating elements; 6—gear wheels; 7—sliding rings; 8—tank with cold water; 9—chiller; 10—electric motor; 11—gear box; 12—rigid steel frame; 13—laser light sheet optics; 14—CCD camera; 15—generator of incense smoke; and 16—pump.

# Mean Flow Patterns Obtained in the Experiments

$\mathrm{Ri}_b = g\alpha\Delta T H_z / U_0^2$

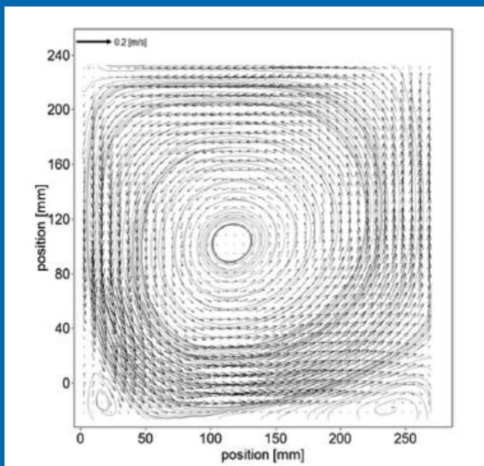


$\Delta T = 0$ K

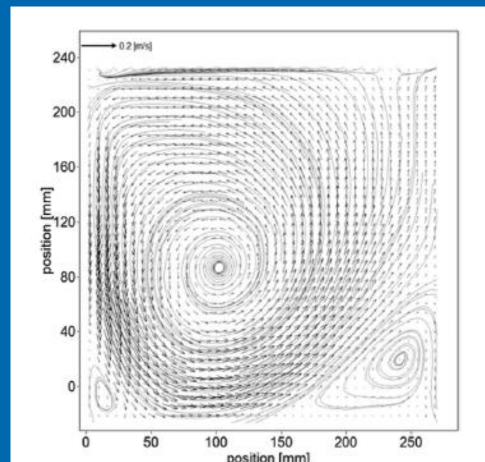


$\Delta T = 11$ K

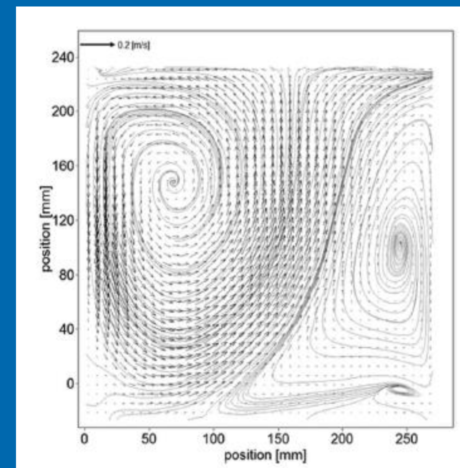


$\Delta T = 21$ K

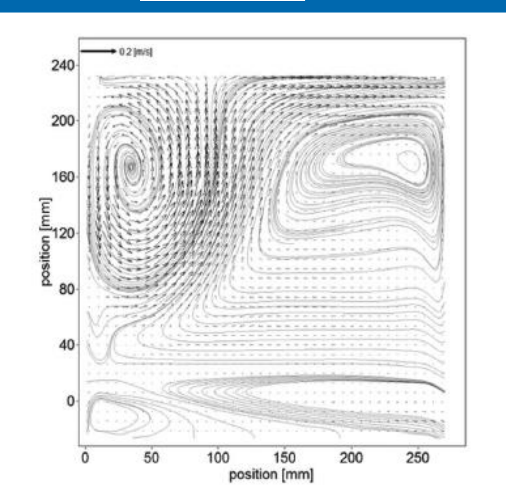


$\Delta T = 33$ K

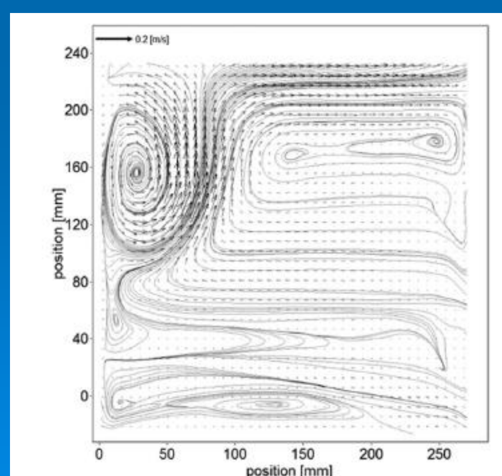


$\Delta T = 44$ K

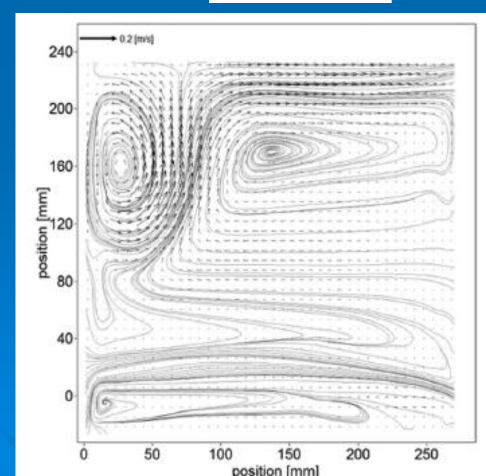


$\Delta T = 54$ K

$(0.19 \leq \mathrm{Ri}_b \leq 0.29)$

# Scalings and Measurements

$$\rho U^2/2 \sim \rho\beta(\delta T)L_z$$

$$L_z \sim U^2/\beta\Delta T$$

$$S = dU_y/dz \sim U_y/L_z$$

$$dU_y/dz \sim U_y\beta\Delta T/U^2 \sim \beta\Delta T/U$$

$$\rho u^2/2 \sim \Pi\ell_z/u_z \sim \ell_z^2 S^2 \sim \ell_z^2(\beta\Delta T/U)^2$$

$$u \propto \ell_z \Delta T$$

$$\dot{\Pi} = \nu_T S^2$$

$$\nu_T \sim \ell_z u_z$$

turbulent $u_z$ (snowflakes)

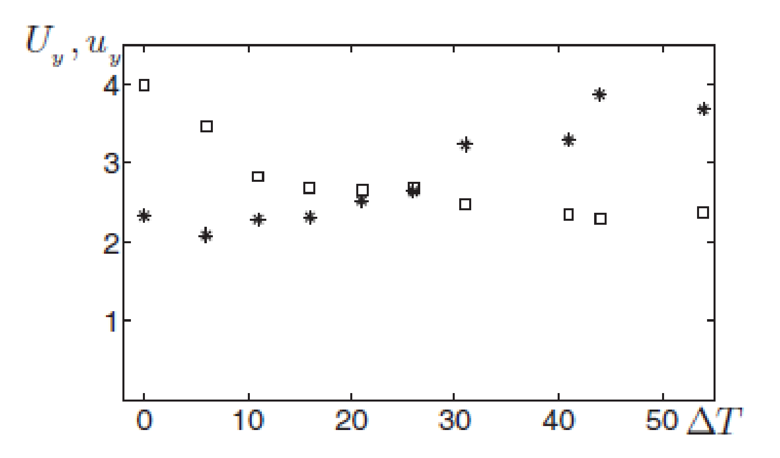


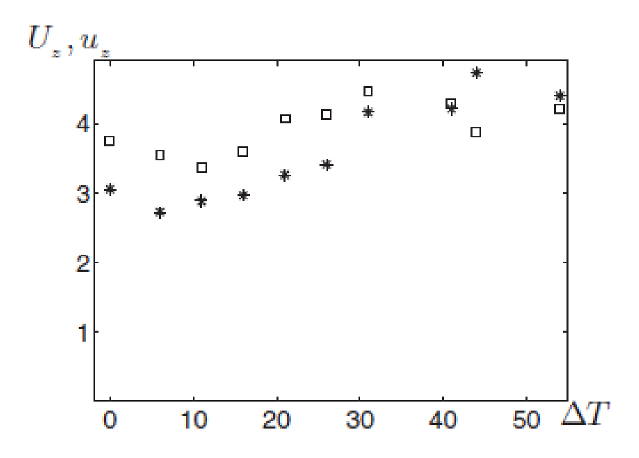

# References


- **Zilitinkevich, S., Elperin, T., Kleeorin, N., and Rogachevskii, I, 2007:** Energy- and flux-budget (EFB) turbulence closure model for stably stratified flows. Boundary Layer Meteorology, Part 1: steady-state homogeneous regimes. *Boundary Layer Meteorology,* 125*,* 167-191*.*

- **Zilitinkevich S., Elperin T., Kleeorin N., Rogachevskii I., Esau I., Mauritsen T. and Miles M., 2008:** Turbulence energetics in stably stratified geophysical flows: strong and weak mixing regimes. *Quarterly Journal of Royal Meteorological Society,* 134, 793-799.

- **Zilitinkevich, S.S., Elperin, T., Kleeorin, V. L'vov, N., Rogachevskii, I., 2009:** Energy- and flux-budget turbulence closure model for stably stratified flows. Part II: the role of internal gravity waves. *Boundary-Layer Meteorol. 133*, 139-164.

- **Zilitinkevich, S.S., Elperin, T., Kleeorin, N., Rogachevskii, I., and Esau, I., 2013:** A hierarchy of energy- and flux-budget (EFB) turbulence closure models for stably stratified geophysical flows. Boundary-Layer Meteorol. 146, 341-373.

- **Eidelman A., Elperin T., Gluzman Y., Kleeorin N., and Rogachevskii I., 2013:** "Experimental study of temperature fluctuations in forced stably stratified turbulent flows". Physics of Fluids, 25, 015111 (1-16).

- **Cohen N., Eidelman A., Elperin T., Kleeorin N., and Rogachevskii I., 2014:** "Sheared stably stratified turbulence and large-scale waves in a lid driven cavity". Physics of Fluids, 26, 105106 (1-16).

- **Elperin T., Kleeorin N., Rogachevskii I., Soustova I.A., Troitskaya Yu., Zilitinkevich S., 2018:** " Internal gravity waves in turbulence closure model for atmospheric stably stratified flows". To be submitted to Phys. Rev. E.

# Conclusions

- Budget equations for the kinetic and potential energies and for the heat flux play a crucial role for analysis of stably stratified turbulence.
- Explanation for no critical Richardson number.
- Reasonable Ri-dependencies of the turbulent Prandtl number, the anisotropy of stably stratified turbulence, the normalized heat flux and TKE which follow from the developed theory.
- The scatter of observational, experimental, LES and DNS data in stably stratified turbulence are explained by effects of large-scale internal gravity waves on SBL-turbulence.

# Conclusions

- ❖Predictions of energy- and flux-budget turbulence closure (EFB) model are in a good agreement with the experimental results.

- ❖Temperature cannot be considered as a passives scalar in most of the range of grid frequencies because Richardson number is small **<u>only</u>** for large frequencies.

- ❖We detected also long-term nonlinear oscillations of the mean temperature in stably stratified turbulence for all frequencies of grid oscillations similarly to the case of the unstably stratified flows.

# THE END